NASA CR-80004

Aerospace Research Center

BEAM ALIGNMENT TECHNIQUES BASED ON THE CURRENT MULTIPLICATION EFFECT IN PHOTOCONDUCTORS

By Raymond P. Borkowski, Robert Carvalho, Joseph C. Scanlon
Aryeh H. Samuel and Daniel Grafstein

SECOND SUMMARY TECHNICAL PROGRESS REPORT
November 1966

Prepared under Contract No. NAS 12-8 by
GENERAL PRECISION, INC.
Aerospace Research Center
Little Falls, New Jersey

for National Aeronautics and Space Administration
Electronics Research Center
Cambridge, Massachusetts

GENERAL PRECISION AEROSPACE
Little Falls, New Jersey

BEAM ALIGNMENT TECHNIQUES BASED ON THE CURRENT MULTIPLICATION EFFECT IN PHOTOCONDUCTORS

By Raymond P. Borkowski, Robert Carvalho, Joseph C. Scanlon
Aryeh H. Samuel and Daniel Grafstein

SECOND SUMMARY TECHNICAL PROGRESS REPORT
November 1966

Prepared under Contract No. NAS 12-8 by
GENERAL PRECISION, INC.
Aerospace Research Center
Little Falls, New Jersey

for National Aeronautics and Space Administration
Electronics Research Center
Cambridge, Massachusetts

RESEARCH CENTER
GENERAL PRECISION INC.
AEROSPACE GROUP
LITTLE FALLS, NEW JERSEY

TABLE OF CONTENTS

ABSTRACT

When two light spots impinge on exactly opposite points of a thin photoconductor, the photocurrent is much greater then when they impinge on disparate points. This is the photoconductive multiplication effect, and the ratio by which the current is increased is the multiplication factor. The potential utility of this effect in space communication and navigation and in information systems is the reason for intensive investigation of the effect. Work previous to that reported here has indicated probable feasibility of these applications.

This report, covering work between 15 November 1965 and 15 October 1966, covers progress in three research areas:

1. Experimental investigations of the effect, including the effects of cell thickness, light intensity, and alternating field, as well as measurements of rise and decay times;
2. Theoretical investigations leading towards an explanation of the effect; and
3. The construction of a breadboard device utilizing the effect for beam alignment.

Additional measurements of the dependence of the photoconductive multiplication factor M (cf. NASA CR-431) on experimental parameters were performed. Measurements of the dependence of M on cell thickness entailed the manufacture of photoconductive cells in this laboratory. By pressing doped CdS powder at 20,000 psi, and subsequently annealing in air at 450° C for 90 minutes, some cells were produced which had reasonably good photoconductivity (though not as good as commercial cells). Spraying and painting techniques were also used, but were less successful. The pressed cells had values of M up to 15. There was an apparent trend to lower M at greater thickness, but individual variations were too great to permit general conclusions.

Absolute calibration of light intensity preceded new measurements of the dependence of M on intensity. The multiplication effect was observed when the light flux on one side of the cell was as low as 2.8×10^{-12} watts. Again, a maximum of M was obtained at roughly equivalent intensity of the two spots. When square-wave alternating potentials are applied to a cell exposed to coincident spot illumination, a trend toward lower M at higher frequency is observed. Results at low ($<$ 1 cps) frequency were irregular.

It was shown that, when a multiplication factor greater than unity is observed, the rise time of the photocurrent is less for coincident spot illumination than for individual spot illumination. Rise times for coincident spot illumination were about 0.1 seconds.

A mathematical model of the photoconductive multiplication effect was constructed. This model could, in principle, describe the observed data on the basis of the geometry of charge carrier deposition, diffusion, recombination, and motion in the electric field. A number of FORTRAN programs were written to obtain calculated values of M. After some difficulty, calculated values of M as large as any experimental value were obtained. An effort to match observed and calculated data was initiated.

A breadboard model of a beam alignment device based on the photoconductive multiplication effect was designed, constructed, and demonstrated. In the course of this work, record values of M (up to 1070) were observed. Measurements based on this model indicated the feasibility of using the effect in space communications.

It is concluded that, while considerable progress has been made toward a better understanding of the effect, experiments with other,especially well characterized,photoconductors are indicated.

LIST OF FIGURES

LIST OF TABLES

I. INTRODUCTION

In 1963, workers at the laboratories of General Precision Aerospace observed that an anomalous photocurrent was produced in cadmium sulfide under the following conditions:

a. The material was a photoconductor (copper and chloride doped).
b. It was in the form of a thin plate or disc.
c. The two large sides were in contact with two transparent electrodes, with a potential drop through the disc.
d. Each side was partially illuminated by a small light spot.
e. The light spots fell on exactly opposite points on the photoconductor.

Under these circumstances, the photocurrent was much greater than when only conditions a to d were satisfied. When the light spots do not impinge on opposite points, the photocurrent (i.e. measured current minus dark current) produced by both spots equals the sum of the photocurrents produced by each spot alone. If we call the latter i_1 and i_2, and the total current produced by both spots i_T, we have, in the case of non-coincidence,

$$i_T = i_1 + i_2$$

But when condition e is fulfilled, one observes

$$i_T = M\,(i_1 + i_2),\ M > 1$$

The factor M has become known as the photoconductive multiplication factor; and the observation that $M > 1$ when conditions a to e are fulfilled is known as the photoconductive multiplication effect.

Previously observed values of M ranged up to 115. In this report several higher values are reported, the highest being 1070. Potential applications of the photoconductive multiplication effect are in the areas of space navigation and communication, pattern recognition, and information retrieval. The interest of NASA's Electronic Research Center has been due to the potential space application. The present contract has had, as the primary application in view, the use of the effect in a beam alignment device, which would keep a receiving station turned towards a moving sender; however, this is only an example of an intended use, and a wider field of applications may well be possible.

Investigation of this effect in doped cadmium sulfide photoconductors has proceeded in this laboratory since 1963, with the latter portion being sponsored under this contract. Much of it has concerned the variation of M as different experimental conditions are varied. The previous Interim Technical Report (NASA CR-431), which covers work done before November 1965, and which will henceforth be referred to as ITR, contains an account of these experiments. In brief, it was found that the value of M is a function of many experimental parameters such as wavelength, field, intensity, spot size, and spot position. It was also found that results are very poorly reproducible from one cell to another. To show some of these dependences of the multiplication factor, four graphs from the ITR are reproduced here. Figure 1 shows the variation of M with wavelength when a fixed wavelength (from a filter) is used for one spot and the wavelength of the other spot is varied by use of a monochromator. Four curves, for four filters, are shown; they exhibit maxima in the same wavelength region. Figure 2 shows the variation of M with the intensity of one spot, that of the other being held constant. Figure 3 shows the variation of M with the size of the spot, total light flux being constant. Note the maxima in each curve. Figure 4 shows the variation of M as the center of one light spot is displaced relative to the center of the other. Here also, a sharp maximum is seen. The continuation of work under Contract NAS 12-8, which is reported on here, had three main aims:

1. Complete the experiments on variation of M with experimental conditions in cadmium sulfide. Particular attention was to be paid to the effect of cell thickness on M. These experiments required the fabrication of cells in our laboratory (unsuccessfully attempted before), and were thus unusually difficult and time-consuming.

FIGURE 1

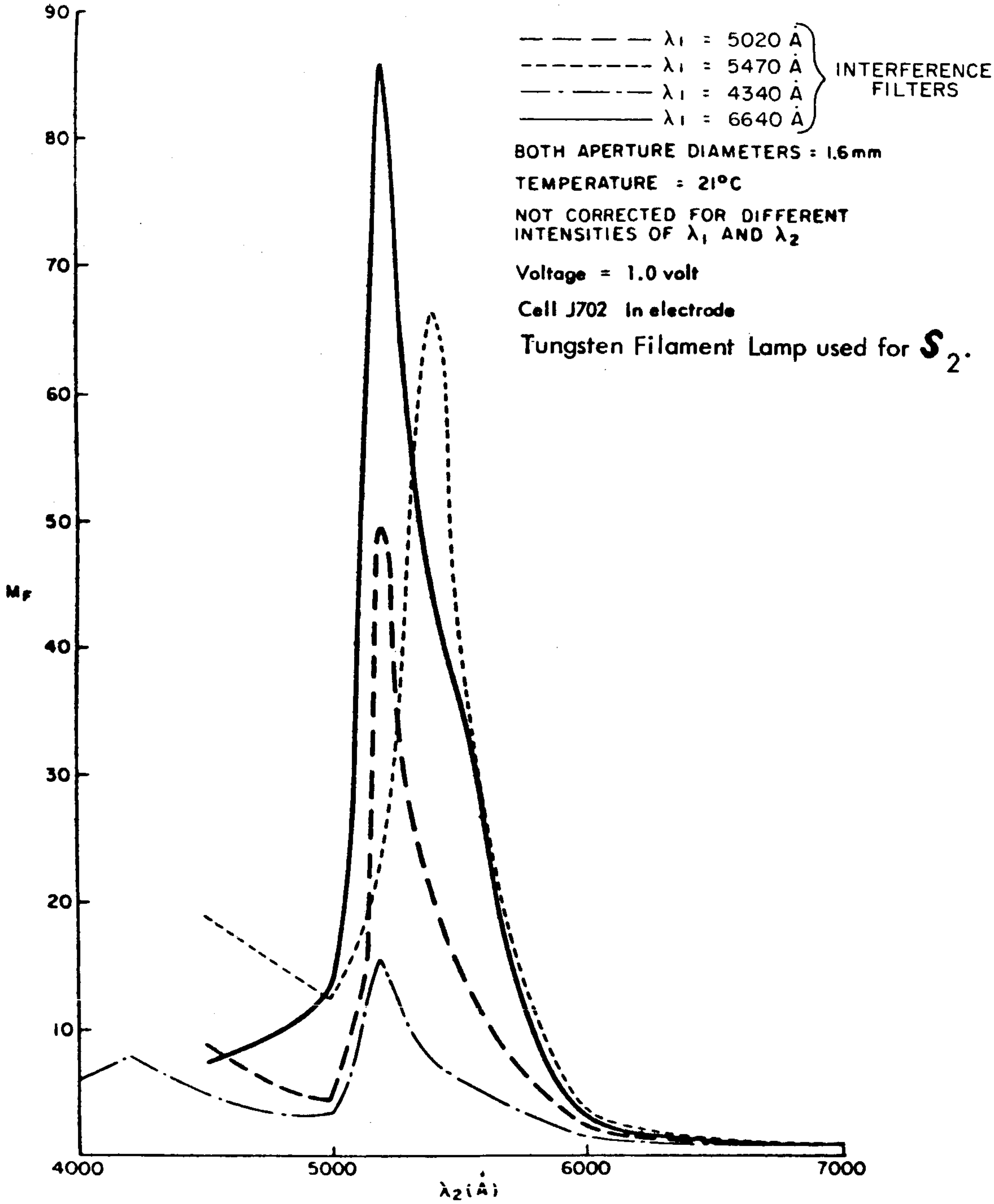

WAVELENGTH DEPENDENCE OF THE MULTIPLICATION EFFECT

Figure 3

Effect of Spot Size on M Defocusing Experiments

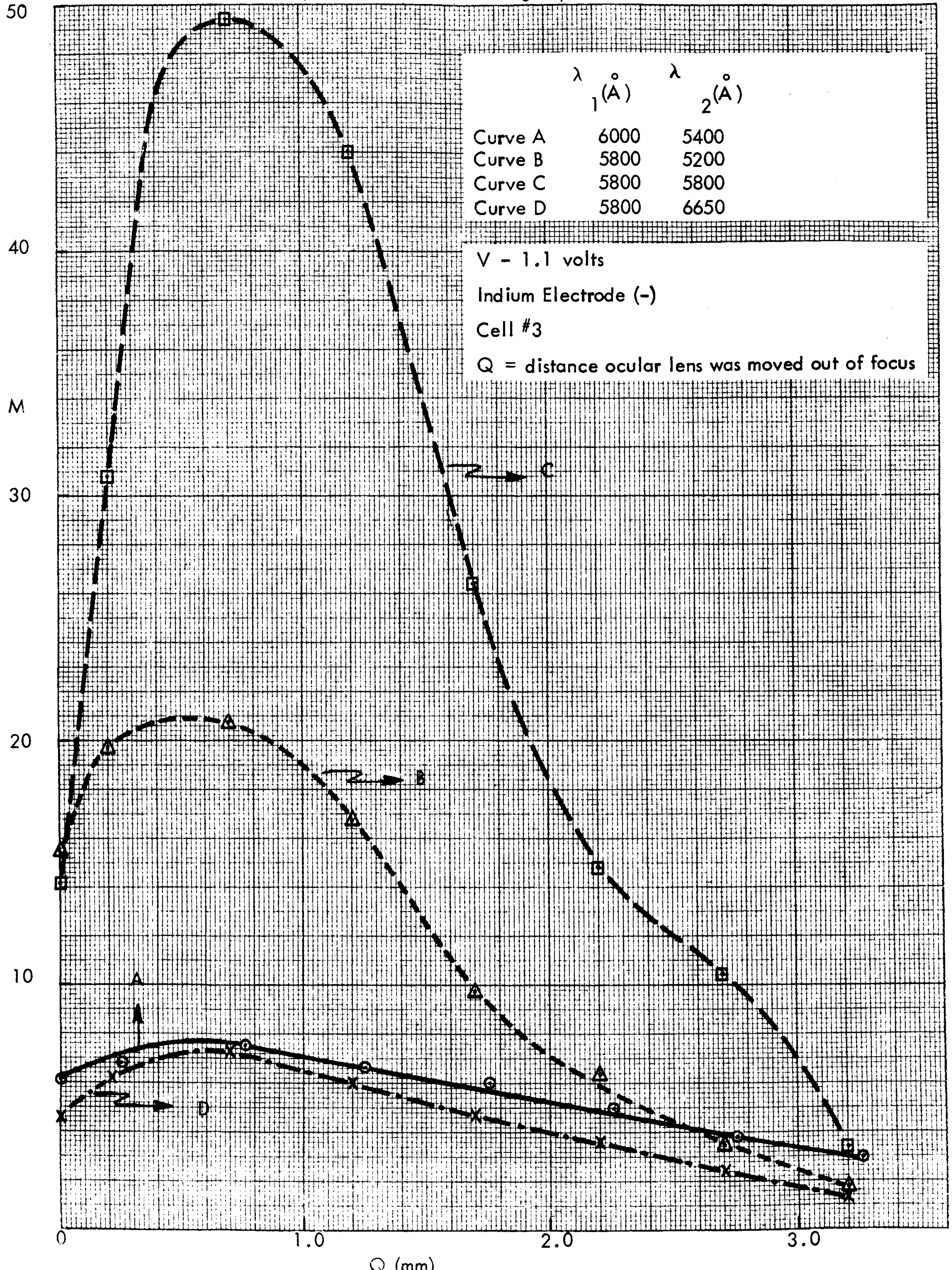

MULTIPLICATION FACTOR AS A FUNCTION OF BIAS PHOTOCURRENT - FIGURE 2

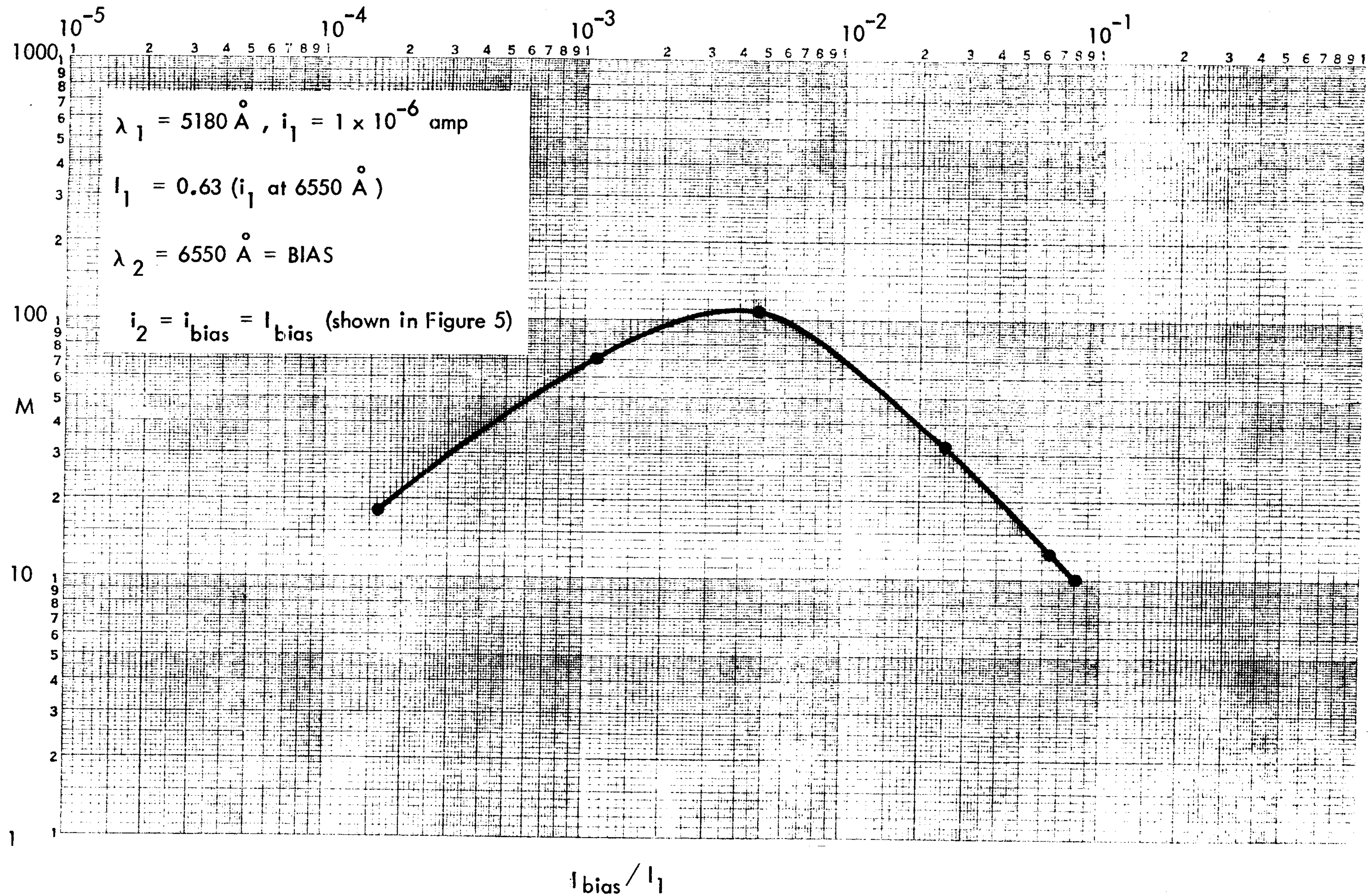

2. Explain the effect in terms of known physical phenomena. To us, this meant the construction of a mathematical model of the effect which could explain observed experiments and predict the results of new ones.

3. Construct a breadboard model of a beam alignment device based on the photo-conductive multiplication effect. This model should not only demonstrate the potential utility of the effect, but should also provide preliminary performance data.

This report covers these directions of investigation. Section II deals with the experimental topics, Section III with the theoretical effort, and Section IV with the breadboard beam follower. Some conclusions are presented in the final section.

This report covers work done under National Aeronautics and Space Administration (NASA) Contract NAS 12-8 at the Aerospace Research Center of General Precision, Inc. during the period 15 November 1965 to 15 October 1966. This research was performed under the supervision of Dr. Daniel Grafstein, Manager, Materials Department, Aerospace Research Center. Participants in the research effort were Dr. Raymond P. Borkowski, Dr. Robert Carvalho, Mr. Robert Flower, Dr. Marvin J. Kornblau, Mr. Casper Olfers, Dr. Aryeh H. Samuel, Mr. Joseph C. Scanlon, and Mr. Clifford Whitmore. Dr. Samuel was the principal investigator. The interest and participation of staff members of the Electronic Research Center of NASA have gone far beyond the requirements of mere financial sponsorship. In particular, we acknowledge the continued interest and frequent suggestions of the contract technical director, Mr. Janis Bebris.

Two papers on work performed under this contract were delivered during the year. In the Appendix, the abstracts of the papers are given as they appeared in the Journal of the Optical Society of America.

II. EXPERIMENTAL RESULTS

A. MULTIPLICATION EFFECT DEPENDENCES

1. Intensity Dependence

Previous results with uncalibrated light sources (see ITR, page 19) indicated that multiplication factors were higher at intermediate than at very high or very low light intensities. In order to relate this dependence to system parameters, it was necessary to determine the dependence of the multiplication effect on absolute light intensities. Therefore two source lamps were calibrated in terms of absolute energy output; for each lamp two different methods were used for calibration. Then the multiplication effect was measured on commercial CdS cells as a function of the intensity of one of the lamps. The experiments are described below.

a. Calibration. Indirect method

The light sources were 100 watt tungsten-filament frosted light bulbs. These were first aged for 50 hours to ensure constant output and then sprayed with black paint so that only a circular aperture at the tip of each bulb was left unmasked. The normal at the center of the aperture was identical with the axis of the bulb. The radius of each aperture was 0.610 cm and the area of each aperture was 1.169 cm^2. The lamps were then calibrated by the Metrology Laboratories at General Precision Aerospace, in comparison with reference standards of the National Bureau of Standards.

When 115 volts was applied across the bulbs, each had a color temperature of 2830° K. The luminosity of the apertures was measured as 28.0 and 27.3 candle power respectively. To ensure that these conditions applied during the experiment, a constant-voltage 115 volt power supply was used to feed the lamp.

From the color temperature, the emission function of the sources as a function of wavelength could be obtained. This is the number of watts per steradian per wavelength interval per cm^2 of tungsten emitting surface emitted at that temperature (the emissivity of tungsten, about 0.94, is already included). If we now multiply this value at each wavelength with the luminosity function (lumens per watt; maximum 680 at 5550Å) and integrate over all wavelengths, we obtain the lumens per steradian per cm^2 or candlepower per cm^2. Comparison with the measured values gives the effective number of cm^2 of tungsten in our source. (This is of course smaller than the actual aperture area since the bulb aperture is not as bright as an actual glowing tungsten surface of the same area and color temperature would be.) It is thus possible to obtain the source output in watts per steradian at any wavelength. The results are given in the next section.

b. Calibration. Direct method

The indirect method of calibration described requires some assumptions about the sources. A better calibration method would be to measure the radiant power directly, rather than calculating the power from the measured luminous intensity. This calibration was accomplished by the more direct method of allowing the light from the source to impinge on a calibrated Eppley bolometer and measuring the output.

The indirect and direct results for the standard lamp (1 cm^2 aperture) in watts per unit wavelength at two wavelengths were:

	Direct	Indirect
545 $m\mu$	3.5×10^{-9}	4.2×10^{-9}
510 $m\mu$	2.8×10^{-9}	3.2×10^{-9}

It is seen that the direct method gave results that were within twenty percent of the results obtained by the indirect method. We consider the direct method to be more reliable.

c. Multiplication factor measurements.

For the redetermination of the intensity dependence of the multiplication effect, absolutely calibrated light sources were positioned on an optical bench. No lenses were used, so that inverse square optics could be taken to apply. A commercial cell (No. G) was mounted in the center of the bench and fitted with masks on each side. The masks contained pinholes whose areas was 1.26×10^{-3} cm^2. The two light sources were mounted 27.0 cm from the pinholes. Both kinds of filters were recalibrated in the Beckman DK-2 spectrophotometer. The angle subtended by the pinhole as seen from the source was 1.48 milliradians.

In these experiments, one source, with a 545 mμ interference filter only, illuminated the indium electrode of the cell. The other source illuminated the glass electrode through a 512 mμ interference filter and neutral density filters having optical densities from zero to 3.0. Thus, the intensity of illumination on the indium was maintained constant, while that on the glass was varied over a factor of 1000. The results of these experiments are given in Table 1.

The light intensity on the indium electrode is 3.5×10^{-9} watts (2.8×10^{-6} watts/cm^2); that on the glass electrode varies from 2.8×10^{-9} watts to 2.8×10^{-12} watts (2.2×10^{-6} to 2.2×10^{-9} watts/cm^2). It is seen that the multiplication factor peaks near 8.9×10^{-10} watts (7.1×10^{-7} watts/cm^2). If the transparency of the indium electrode is near 10-20% , the peak occurs when the intensities on both sides are roughly equal.

In Figure 5 the multiplication factor is plotted against the intensity of the source.

These results confirm previous findings which indicate that the multiplication factor goes through a maximum as the intensity of light on one sides is increased, the other being held constant. These results also show the very considerable gain in sensitivity produced by coincident spot illumination. A flux of 2.8×10^{-12} watts of 512 mμ light, or 7.2×10^6 photons per second, is sufficient to multiply by a factor of 3.5 the photocurrent obtained from a flux of 3.5×10^{-9} watts impinging on the other side.

2. Response to Alternating Bias Voltage

In order to determine whether the multiplication factor is affected by an alternating bias voltage, a sophisticated optical bench was set up and the relationship between the frequency of the impressed field and the multiplication factor was investigated. A low frequency signal generator with a 0-30 volt and 0.1-1000 cps output, was substituted for the battery-helipot system. A square wave was applied to the cell which effectively switched the polarity of the bias voltage periodically. Commercial cell "G" was again selected for testing and equipped with a shielded cable to reduce extraneous pickup.

A Keithley microvolt-ammeter was used to measure the currents.

FIGURE 5

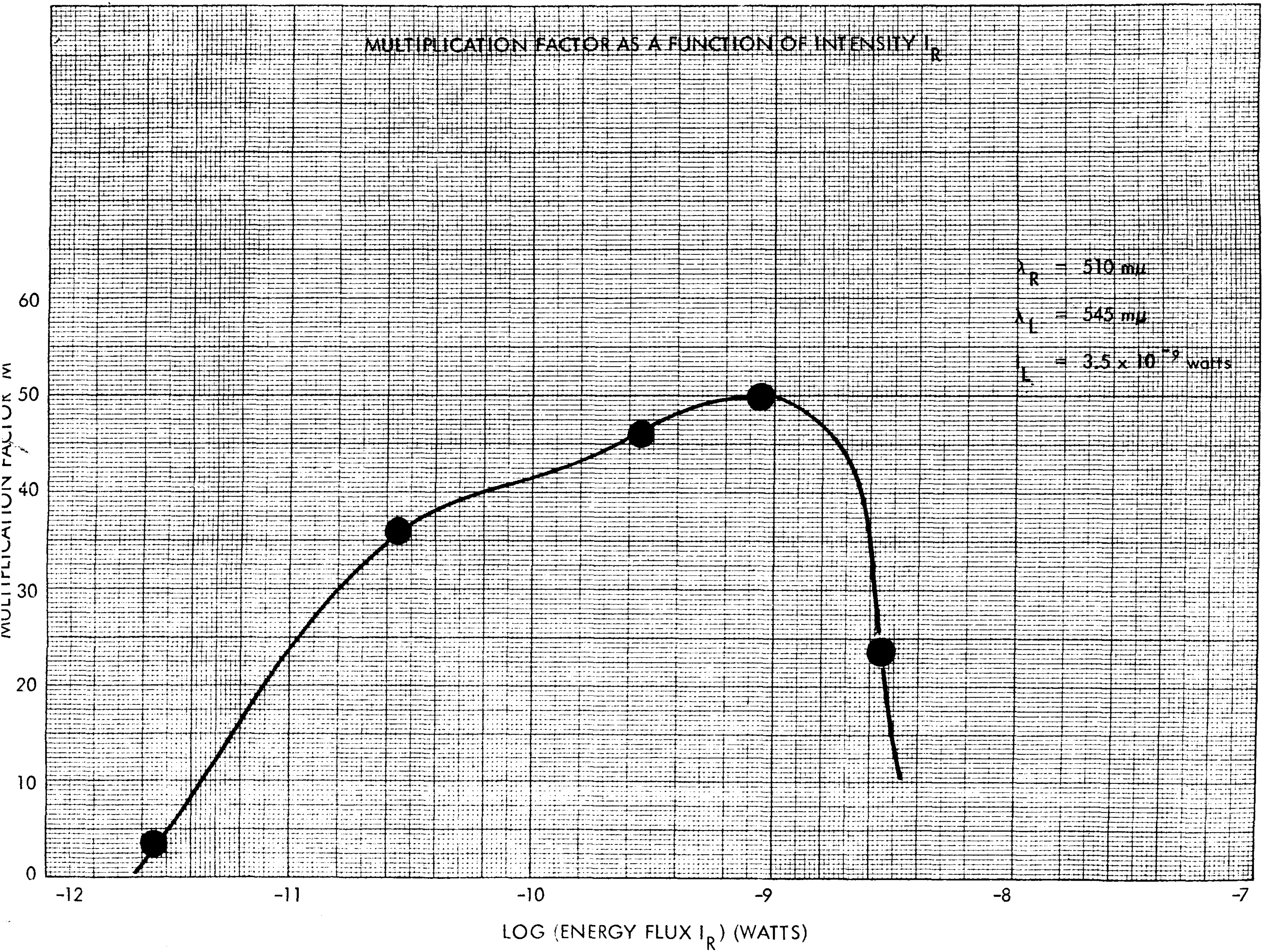

MULTIPLICATION FACTOR AS A FUNCTION OF INTENSITY I_R
λ_R = 510 mμ
λ_L = 545 mμ
I_L = 3.5 x 10^{-9} watts
MULTIPLICATION FACTOR M
0
10
20
30
40
50
60
-12
-11
-10
-9
-8
-7
LOG (ENERGY FLUX I_R) (WATTS)

TABLE 1

DEPENDENCE OF MULTIPLICATION FACTOR ON SOURCE INTENSITY

I_L		I_R^o	OD	I_R		M
3.5×10^{-9} watts	2.8×10^{-6} w/cm^2	2.8×10^{-9} watts	0	2.8×10^{-9} watts	2.2×10^{-6} w/cm^2	23.5
3.5×10^{-9}	2.8×10^{-6}	2.8×10^{-9}	0.5	8.9×10^{-10}	7.1×10^{-7}	50.
3.5×10^{-9}	2.8×10^{-6}	2.8×10^{-9}	1.0	2.8×10^{-10}	2.2×10^{-7}	46.
3.5×10^{-9}	2.8×10^{-6}	2.8×10^{-9}	2.0	2.8×10^{-11}	2.2×10^{-8}	36.
3.5×10^{-9}	2.8×10^{-6}	2.8×10^{-9}	3.0	2.8×10^{-12}	2.2×10^{-9}	3.5

I_L Energy flux from left-hand source through 546 mμ filter

I_R^o Energy flux from right-hand source through 512 mμ filter

OD Optical density of neutral filter inserted on right

I_R Energy flux from right-hand source through 512 mμ filter and neutral filter

M Multiplication factor

Illuminated area 1.26×10^{-3} cm^2

Figure 6 shows the multiplication factor as a function of frequency for several series of experiments. Table 2 gives the values of photocurrents and of the multiplication effect observed under the following conditions: bias voltage ± 1V (square wave), wavelengths: 514 and 520 mμ.

The values given in Table 2 correspond to the Curves (2) and (4) in which the nanoampere scale of the Keithley was used.

Curves (3) and (6) are the results of otherwise similar experiments using the microampere scale of the Keithley.

Curves (1) and (5) correspond to (2) and (4) when repeated a day later.

Curves (1) - (3) represent the A phase (Indium negative) and Curves (4) - (6) represent the B phase (Indium positive).

Figure 7 is similar to Figure 6 except that the left light signal (514 mμ) is <u>not</u> modified by a 2.0 neutral density filter, so that the optical signal is stronger. This gives smaller multiplication values for the frequencies measured.

Note that because of the change of field direction the absolute value of the multiplication has been defined:

$$M = \left| \frac{i_T - i_D}{i_L + i_R - 2i_D} \right|$$

Consideration of the data reveals the following:

a. The multiplication effect is observed throughout the frequency range.

b. Above 0.1 cps the reproducibility is poor for the low light intensity measurements.

c. There is a possible maximum value of M at 1.0 cps at low light intensities. This maximum - if real - may be related to the rise times of the cell which are in the 0.1 to 1 second region.

d. There is a polarity dependence which is particular strong at low light intensities. The greater values of M found when the indium electrode is negative suggest the presence of a blocking electrode.

TABLE 2

MULTIPLICATION EFFECT FOR ALTERNATING SQUARE WAVE BIAS VOLTAGE

ν	Phase	i_D	i_L	i_R	i_T	$\lvert M\rvert$
0.01	A	-5	-5	-10	400	81
	B	-5	1	-6	-20	3
0.10	A	-5	-5	-10	400	81
	B	-5	2	-3	-14	1
1.00	A	-5.5	-3	-8.5	400	810
	B	-5.5	-1	-6.5	-5	0
10.0	A	-6	-3	-7.5	(190)	131
100	A	-6.5	(-4)	(-10)	(175)	182
1000	A	-6.5	(-4.5)	(-10)	(165)	114

i_D = dark current; i_L, i_R = currents for single-side illumination; i_T = current for two-side illumination. All units in nanoamperes (10^{-9} amp). ν = frequency of square wave oscillator. E = 1 volt (amplitude of square wave oscillator). λ_L (514 mμ) impressed on CdS side of cell. λ_R (520 mμ) impressed on In side of cell. Neutral density filter 2.0 inserted on left side of bench.

Phase A: Indium negative, CdS positive.
Phase B: CdS negative, In positive.

$|M|$ is defined as $$\left|\frac{i_T - i_D}{(i_L - i_D) + (i_R - i_D)}\right|$$

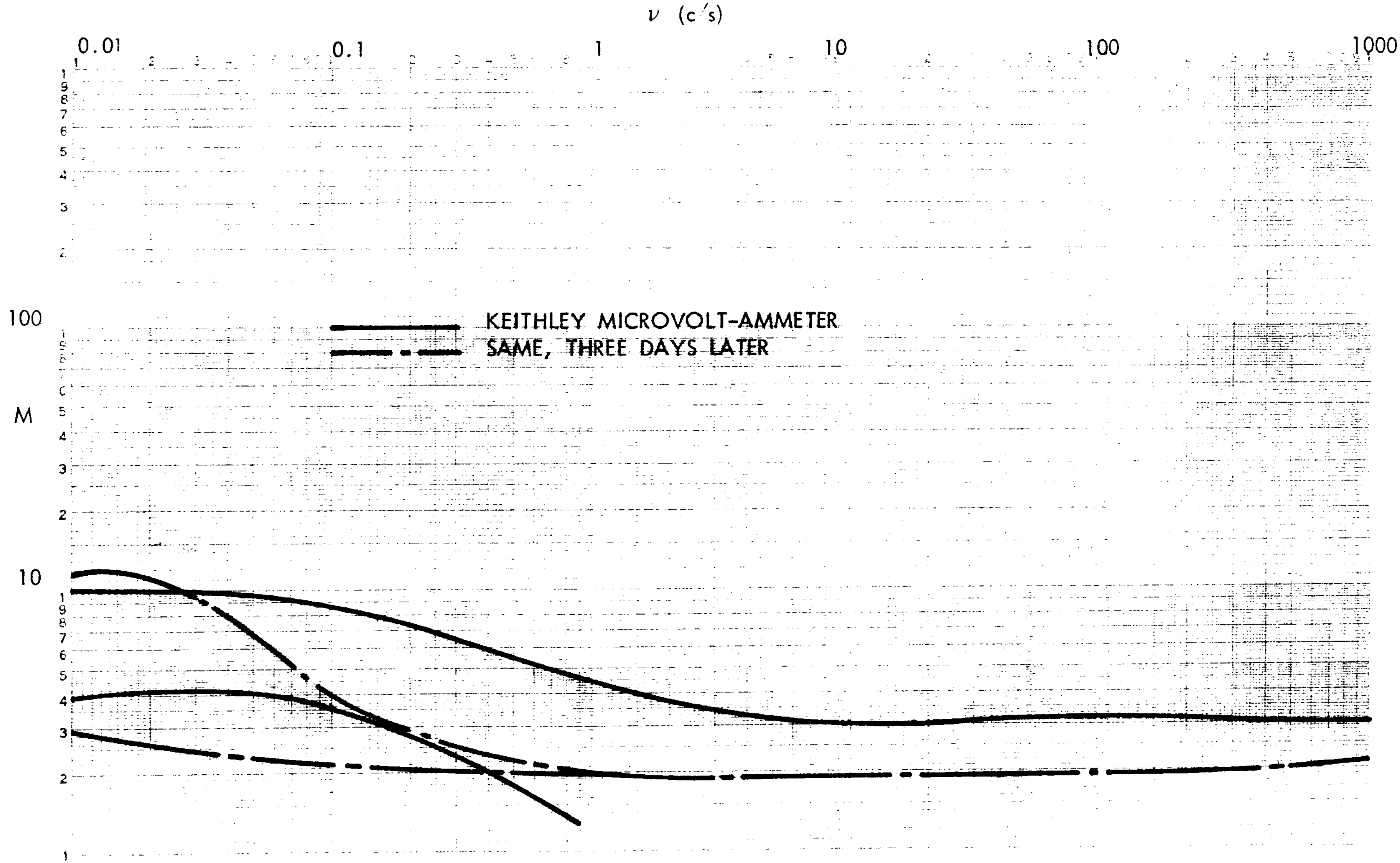

FIGURE 7

MULTIPLICATION FACTOR AS A FUNCTION OF FREQUENCY AT HIGH LIGHT INTENSITY

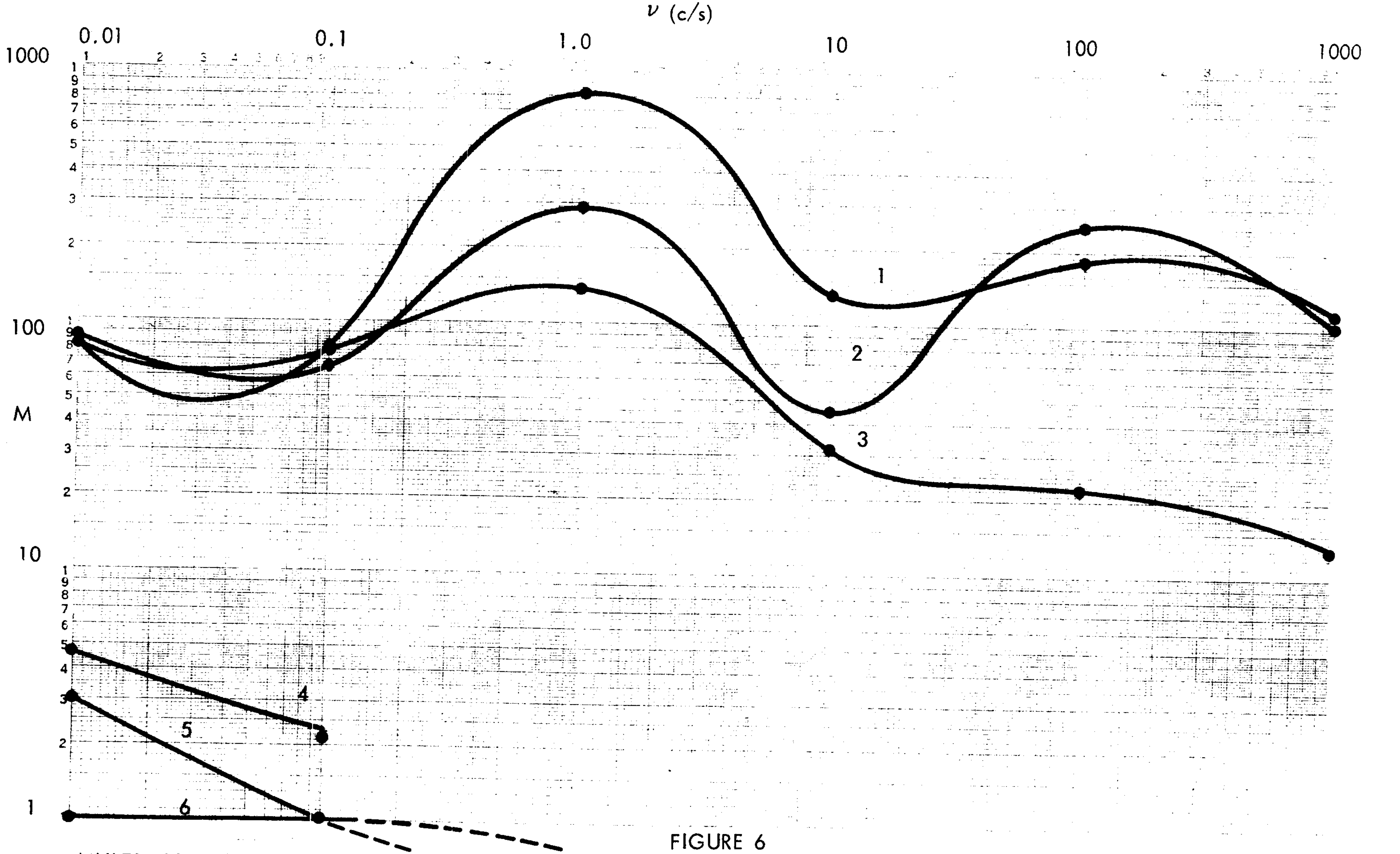

FIGURE 6
MULTIPLICATION FACTOR AS A FUNCTION OF FREQUENCY - LOW LIGHT INTENSITY - VARIOUS MEASURING INSTRUMENT

3. Study of Rise and Decay Times

a. Previous results

The results of the rise and decay times studies reported in the ITR have been shown to be incorrect.

In the earlier studies the oscilloscope was connected to the output of a Keithley 150A electrometer which was placed in series with the photocells. In checking the characteristics of the electrometer, both from the manufacturers specifications and by an independent method, the response time of the meter was determined to lie in the range 0.5-1.0 second. Since the rise times measured were of a comparable magnitude, their validity was suspect. Thus we adopted the measuring circuit shown in Figure 8. With this new circuit the rise times have been found to be significantly less than were reported in the ITR. It is therefore felt that the earlier results should be rejected.

b. Single side illumination

In carrying out these experiments, a camera shutter, whose rise time was at most 20 milliseconds, was employed. The vertical amplifier risetime for the 536 oscilloscope was quoted by the manufacturer to be 0.03 microseconds. Thus neither the shutter nor the oscilloscope would interfere with the risetime measurement of the photocell, which is expected to be of the order of 50-100 milliseconds. Masks, whose areas were approximately 2×10^{-3} cm^2, were used on both sides of the photocell. A Bausch and Lomb high intensity monochromator was used to isolate the various wavelengths, and a bias voltage of 1.0 volt was applied for all the results reported here. The rise times were calculated from the oscillographs. They are defined as being the time the photocell requires to achieve 50% of its steady state photocurrent. The results are given in Table 3 for single-sided illumination of a commercial cell.

We see first that the rise times are at least five times greater than the shutter speed, so that these values should correspond to the rise time of this particular photocell. The rise time between 5500-6750Å, is about 150 milliseconds and increases as one proceeds to

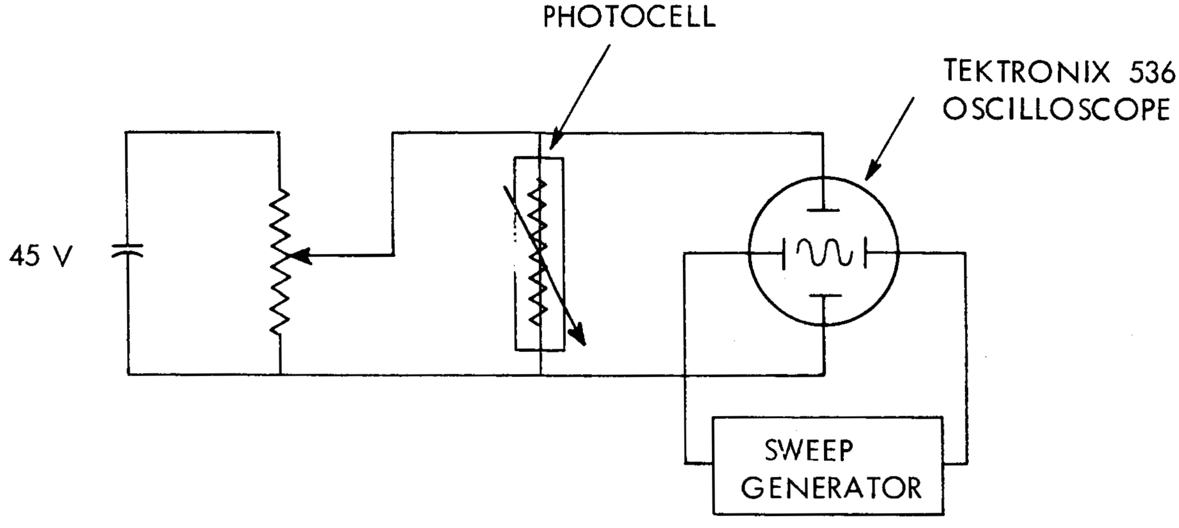

ELECTRICAL CIRCUIT FOR MEASURING RISE AND DECAY TIMES

FIGURE 8

shorter wavelengths. An indication of the reproducibility of the results can be obtained by comparing the results of the experiments where the indium electrode is negative and the glass electrode is positive. A rather close correspondence is noted indicating that the rise time is independent of the electrode illuminated. The intensity of light reaching the CdS should be less on the indium side than on the glass side. No effect of this intensity difference is seen.

c. Opposite side illumination

To measure rise times when two beams impinge on opposite sides, the first requirement was an optical system which turns on the two beams simultaneously. The system used is shown in Figure 9. The two beams pass through the center of the same shutter, and are turned on and off within 10 milliseconds of each other.

Tables 4 and 5 show the results obtained with this experimental arrangement. Because of the longer path length, it was found that light intensities were 7.5 times lower than for the previous arrangement. Thus, the single side rise times τ_{r_1} and τ_{r_2} are greater than those of Table 3. The two-side rise times are considerably lower than the single-side ones, especially when M is considerably above unity.

On the other hand, when there is little or no multiplication, the rise time for simultaneous illumination is equal to the faster of the two single-side illumination rise times.

The decay times for both single-side and dual-side spot illumination were at least as fast as the shutter speed, that is 20 milliseconds or less, so that no comparison was possible.

d. Partial illumination and full surface illumination

Earlier observations had shown that little or no multiplication occurred when opposite surfaces of the photocell were completely illuminated. The fact that no multiplication was observed when the rise time for single-side illumination was 100 milliseconds or less suggested a comparison of the rise times for partial and full surface illumination. These experiments were conducted under conditions of constant intensity. The results are summarized in Table 5. The glass electrode was illuminated in both cases. It was possible to measure the decay times and these are included also.

TABLE 3

RISETIMES AT VARIOUS WAVELENGTHS FOR CELL No. 4

A. Indium Electrode Illuminated

λ (Å)	τ_R (seconds)	
	In (+)	In (-)
5100	0.40	0.60
5200	0.25	0.42
5250	0.19	0.33
5300	0.18	0.26
5500	0.13	0.38
5750	0.10	0.12
6000	0.08	0.08
6250	0.09	--
6500	0.11	0.10
6750	0.15	0.12

B. Glass Electrode Illuminated

λ (Å)	τ_R (seconds)	
	Glass (+)	Glass (-)*
5100	0.52	---
5200	0.40	
5250	0.32	
5300	0.39	
5500	0.22	
5750	0.20	
6000	0.20	
6250	0.16	
6500	0.16	
6750	0.18	

τ_R = Rise Time

* = Unable to measure rise time when glass electrode was illuminated and negative because signal was not large enough to be seen on oscilloscope.

TABLE 4

RISE TIMES FOR SIMULTANEOUS ILLUMINATION OF BOTH ELECTRODES

Cell No. 4

λ_1 ($m\mu$)	λ_2 ($m\mu$)	τ_{r_1} (sec)	τ_{r_2} (sec)	$\tau_{r(1+2)}$ (sec)	M
512	520	1.9	0.91	0.26	3.6
512	580	1.3	1.04	0.28	2.7
512	650	1.35	0.70	0.40	1.8
575	520	0.45	1.55	0.25	1.3
575	580	0.38	1.0	0.13	1.3
575	650	0.40	0.58	0.25	1.15
633	520	0.09	1.1	0.10	1.11
633	580	0.10	1.0	0.10	1.07
633	650	0.08	0.71	0.10	0.98

λ_1 = wavelength illuminating indium electrode using interference filter.

λ_2 = wavelength illuminating glass electrode using monochromator.

$A_1 = A_2$ = aperture areas = 2×10^{-3} cm^2.

Voltage = 1.0 volt

τ_{r_1} = rise time obtained by illuminating indium electrode

τ_{r_2} = rise time obtained by illuminating glass electrode

$\tau_{r(1+2)}$ = rise time obtained for simultaneous illumination of both electrodes

TABLE 5

COMPARISON OF RISE TIMES FOR PARTIAL AND FULL SURFACE ILLUMINATION

Cell No. 4 | Indium Electrode (-) | V = 1.0 volt

λ ($m\mu$)	A_p			A_f		
	τ_r(msec)	τ_d(msec)	i_s(mv)	τ_r(msec)	τ_d(msec)	i_s(mv)
512	170	4*	134	70	40	780
645	6*	60	590	2.5*	60	840

A_p = partial illumination area $\approx 2 \times 10^{-3}$ cm^2

A_f = full illumination area $\approx$ 1 cm^2

τ_r = rise time

τ_d = decay time

i_s = steady state signal (millivolts on the oscilloscope, roughly equivalent to nanoamperes in the cell).

* = these values are in the range of the shutter rise time.

OPTICAL SYSTEM FOR RISE TIME STUDY OF SIMULTANEOUS OPPOSITE SURFACE ILLUMINATION

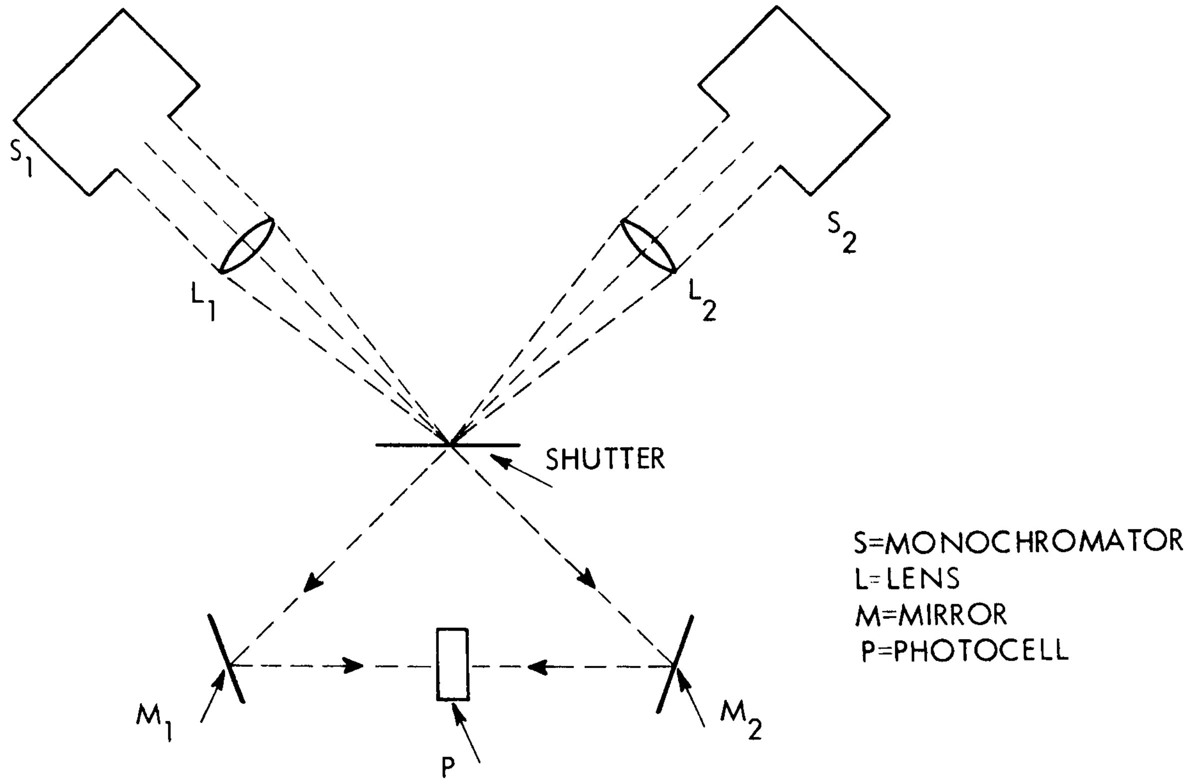

FIGURE 9

The rise time was smaller (a faster response) for full surface illumination than for partial illumination, whereas the decay process was slower (at least for 512 mμ light). From these data two conclusions are drawn. First, the rate at which the steady state condition (the plateau region of the rise time curve) is established depends on the number of charge carriers initially produced, before any recombination or trapping processes take place. This rate is faster when the number of charge carriers initially produced is large, which is the case for full surface illumination. Secondly, the rate of decay is dependent on the steady-state concentration of free charge carriers, diminishing as this number increases. (The decay time then grows with the steady-state concentration of carriers.)

Since the intensity was maintained constant, the increase in the steady-state photocurrent (as shown by the i_s values in Table 5 is attributed to an increase in the area of illumination.

Approximately 500 times more area was illuminated in the full-surface case than in the partially illuminated case. The steady-state photocurrents, on the other hand, only increased by a factor of approximately 6, using 512 mμ light, and a factor of approximately 1.4, using 645 mμ light. Thus, the steady-state photocurrent was not a linear function of the area of illumination.

These experiments on rise and decay times indicate a roughly inverse correlation between photocurrent and rise time. As a result, when M is substantially greater than unity, the rise time when both cell sides are illuminated is considerably less than the lesser of the one-side illumination rise times (Table 4). This is not seen when $M \approx 1$. This effect has been used in star trackers.

Thus, if we calculate the ratio min $(\tau_{r_1}, \tau_{r_2})/(M\tau_{r(1+2)})$ for the data of Table 4, values between 0.8 and 1.4 are obtained for all experiments except one which gives 2.25.

B. FABRICATION OF PHOTOCELLS: THE EFFECT OF CELL THICKNESS ON M

Our initial unsuccessful attempts to fabricate photoconductive cells from homemade doped CdS powder were described in the First Interim Progress Report (pp. 3-9). It was decided to use a commercially available photoconductive powder in the cell fabrication program.

A doped cadmium sulfide powder which was alleged to be photoconductive, was purchased from Sylvania Electronic Products, Inc. The powder was designated "PC-103 Photoconductor Material, Lot No. PC-103-14" by the manufacturer. Using this material, cells were fabricated in two ways - by pressing the dry powder into pellets and by spray deposition of a xylene suspension of the powder.

None of the spray deposited cells were found to exhibit photoconductivity so we will not consider this method any further in this report. The work with the pressed pellet cells is described below.

1. Fabrication Methods

Pellets were prepared by placing an appropriate amount of material in a pellet press, evacuating the chamber and then applying a pressure of 20,000 p.s.i. Discs of varying thicknesses and 13 mm diameter were prepared in this manner.

Initial screening of the cells was accomplished by measuring the photosensitivity, i.e., the ratio of the electrical resistance of the cell in the dark to that under illumination (R_D/R_L). It was found that sintering of the cells was necessary to produce photosensitivities greater than 3. Experiments were carried out in an attempt to relate photosensitivity to sintering conditions. The results of the sintering experiments may be summarized as follows:

a. Sintering in air improved the photosensitivity of the pellet cells.
b. The highest photosensitivities ($R_D/R_L \approx 1000$) were obtained at sintering temperatures around 440° C.
c. The photosensitivity achieved by sintering is unpredictable varying from 50 to 1500.
d. Sintering in vacuo and in N_2 atmospheres did not improve photosensitivity.

High values of the cell resistance under illumination ($R_L \geq 5 \times 10^5$ ohms) suggested that the resistance of the cell measured in the light is limited by the contact resistance between the pellet surface and the conducting glass which was used to make electrical contact with the pellet. Experiments indicated, however, that because of the complicated

TABLE 6

MULTIPLICATION FACTOR AS A FUNCTION OF ELECTRIC FIELD

CELL GP-2

Thickness (d) = 1.0 mm

λ_L = 514 mμ; λ_R = 650 mμ

Voltage (volts)	amperes (x 10^9)				M
	i_D	i_L	i_R	i_T	
4.5	0.80	0.80	1.4	5.2	7.3
9.0	1.00	1.10	2.6	14.0	7.6
17.5	1.40	1.55	6.25	36.5	7.0
24.6	1.80	2.1	11.0	64.0	6.55
32.0	2.60	3.1	17.0	94	6.13
40.0	3.70	4.2	22.2	127	6.5

TABLE 7

MULTIPLICATION FACTOR VARIATION WITH WAVELENGTH COMBINATION

CELL GP-2

Thickness (d) = 1.0 mm

V = 4.5 volts

amperes (x 10^9)

λ_L (mμ)	λ_R (mμ)	i_D	i_L	i_R	i_T	M
Unfiltered	600	0.63	12.0	0.75	130	11.2
547*	600	0.48	0.51	0.64	1.2	4.5
664*	600	0.46	0.57	0.65	4.0	11.8

*Interference filters

λ_R is illuminating positive electrode in above experiments.

non-ohmic behavior of the cell resistances, it would not be feasible to attempt to separate the effect of contact resistance from the true cadmium sulfide resistance.

2. Multiplication Effect in Pressed Pellet Cells

Approximately forty cells were fabricated by the pressing techniques with cell thicknesses ranging from 0.2 mm to 5 mm. Of these, six were shown to exhibit a multiplication effect large enough to be measurable with our instruments. The experiments that were carried out with these six cells are described below.

a. Cell GP-2

Cell GP-2 was approximately 1 mm thick. Its initial photosensitivity was 167. Before checking the pellet for the multiplication effect, its photosensitivity was rechecked, as it had been standing in the air for about three weeks. The photosensitivity (ratio of dark to light resistance) had decreased to 14. Previous workers have reported a reduction of the photosensitivity because of the absorption of moisture and have recommended a baking process to drive off the moisture. Cell GP-2 was therefore subjected to a temperature of 105° C for three hours. No improvement in the photosensitivity was noted.* It was also observed that the photocell reacted rather slowly to light. The photocell was then checked for the multiplication effect. First, the effect of field was investigated for a fixed wavelength combination. The results are given in Table 6. Next, experiments were conducted in which the wavelength combination was varied. These results are given in Table 7. The maximum multiplication factor achieved with cell GP-2 was 11.8.

b. Cell GP-3A

This 0.47 mm cell had indium deposited on one face. Only a single measurement of M(=2.5) was made because the photocurrents obtained by illuminating the indium coated face were low. Data are given in Table 8B.

* Later experiments with other cells indicated that evacuation at ca. 10^{-3} torr improved the photosensitivity.

TABLE 8

A. GP-8 Thickness = 0.97 mm
R_D = 10^9 ohms
R_L = 9×10^5 ohms

$\times 10^9$ amperes

λ_L(m)*	λ_R(m)+	V	i_D	i_L**	i_R**	i_T**	M
664	600	1.0	2.5	5.0	3.5	9.8	2.1
664	600	2.0	7.5	15.0	10.0	34.0	2.65
664	600	3.2	14.5	29.0	21.0	82.0	3.2
664	600	4.5	21.0	41.0	30.	110.	3.0
Unfiltered	600	3.2	15.5	140.	23.5	420.	3.05
547	500	3.2	15.5	36.	21.	79.	2.4
520	500	3.2	15.5	39.	21.	94.	2.7
502	500	3.2	15.0	32.	22.	68.	2.2

* Interference Filters
** Not corrected for dark current
\+ Monochromators

B. GP-3A Thickness = 0.47 mm
$R_D > 10^9$ ohms
$R_L = 9 \times 10^5$ ohms

Layer of Indium evaporated on one surface

$\times 10^9$ amperes

λ_L*	λ_R(mμ)	V (volts)	i_1	i_2	i_T	M
Unfiltered	650	1.0	0.09	0.8	2.25	2.52

* Illuminating indium electrode
Currents corrected for dark current.
Discontinued any further experimentation on this pellet because photocurrents obtained by illuminating indium layer were very low with unfiltered light.

c. Cell GP-4A

This 1.58 mm cell had indium deposited on one of its flat surfaces. The data appear in Table 9B.. The largest multiplication factor observed was 15.1. This was the largest multiplication factor obtained in all the home-made cells.

d. Cell GP-8

This cell was made approximately the same thickness as GP-2 (1 mm). The largest value of M that was found for GP-8 was 3.2. See Table 8A .

In Table 10, cells GP-2 and GP-8 are compared in terms of their M values under similar conditions. It is seen that although these cells have the same thickness, the multiplication factor for GP-2 is about four times greater than that of GP-8. Also, the postulate that the multiplication effect is related to the magnitude of the photosensitivity seems to be refuted as GP-2 has a much lower value of R_D/R_L than that of GP-8.

e. Cell GP-16

This is the thickest of the pellet cells that showed a multiplication effect; thickness (d) = 2.40 mm. The data for this cell are given in Table 9. . The largest value of M was only about 2.5.

f. Cell GP-17

Only a single measurement was made on this cell, yielding a multiplication factor of 2.8. See Table 11.

g. Parameter dependences

In Table 11, cells GP-16 and GP-17 are compared under similar conditions. These experiments were designed to determine the variation of M with thickness. It is seen that GP-16, which is twice as thick as GP-17, has a M value only two-thirds that of GP-16. Furthermore, if we compare GP-16 and GP-4A (see Table 9), again it is seen that the thinner GP-4A cell has the greater M value by a factor of five or more. However, in this case the indium layer on GP-4A may be influencing the effect by reducing the contact resistance.

TABLE 9

MULTIPLICATION FACTORS UNDER VARIOUS CONDITIONS FOR SINTERED PELLETS

A. Pellet GP-16 d=2.40 mm V- 40 volts

1. Full Surface Illumination - Left electrode negative.

x 10^9 amperes

$\lambda_L(m\mu)$	$\lambda_R(m\mu)$	i_D	i_L	i_R	i_T	M
Unfiltered	500	1.6	3.6	2.4	7.6	2.14
Unfiltered	550	1.7	4.0	3.1	9.3	2.05
Unfiltered	650	1.7	4.1	2.8	8.5	1.94

2. Spot Illumination - Left electrode negative.

$\lambda_L(m\mu)$	$\lambda_R(m\mu)$	i_D	i_L	i_R	i_T	M
Unfiltered	550	1.5	2.4	2.0	4.0	1.79*
Unfiltered	550	1.3	2.2	1.5	3.9	2.45**
Unfiltered	650	1.1	1.9	1.4	3.5	2.18**

* - Spots non-aligned; centers approximately 6 mm apart.
** - Spots aligned.
i_L, i_R and i_T have not been corrected for the dark current.

B. Pellet GP-4A d=1.58 mm Indium electrode on one surface (left electrode)
V=40 volts Spot Illumination

1. Indium electrode positive

x 10^9 amperes

$\lambda_L(m\mu)$	$\lambda_R(m\mu)$	i_D	i_L	i_R	i_T	M
Unfiltered	500	2.1	3.7	2.2	19.5	10.2
Unfiltered	520	2.25	4.2	2.4	26.5	11.5
Unfiltered	550	2.3	4.3	2.8	26.5	9.7
Unfiltered	650	2.2	4.1	2.4	33.0	14.7

2. Indium electrode negative

$\lambda_L(m\mu)$	$\lambda_R(m\mu)$	i_D	i_L	i_R	i_T	M
Unfiltered	650	0.6	0.65	2.5	30.0	15.1

TABLE 10

GP-2 Thickness = 1.0 mm.

GP-8 Thickness = 0.97 mm.

Pellet	V (volts)	$\lambda_L{}^*$ ($m\mu$)	$\lambda_R{}^+$ ($m\mu$)	i_D	i_L	i_R	i_T	M
GP-2	4.5	664	600	0.46	0.11	0.19	4.0	11.8
GP-8	4.5	664	600	21.0	20.0	9.0	89.0	3.0
GP-2	4.5	Unfiltered	600	0.63	11.37	0.12	129	11.2
GP-8	3.4	Unfiltered	600	15.5	125	8.0	405	3.0

* Interference Filters

\+ Monochromator

i_L, i_R, and i_T have been corrected for the dark currents.

TABLE 11

MULTIPLICATION FACTOR FOR TWO CELLS OF DIFFERENT THICKNESS

λ_L = Unfiltered Light

λ_R = 633 mμ

V = 40 volts

Spot Illumination

Pellet	d(mm)	i_D	i_L	i_R	i_T	M
		$\times 10^9$ amperes				
GP-17	1.16	3.0	6.5	3.5	14.0	2.75*
GP-16	2.40	0.18	0.18	0.54	0.85	1.86*
GP-16	2.40	0.28	0.47	0.37	0.92	2.29**

*λ_L = illuminating negative electrode

**λ_L = illuminating positive electrode

Neither the wavelength nor the polarity appears to have a strong influence on M in these homemade pellets. For the symmetrical cells, the absence of any effect of polarity is to be expected. For pellet GP-4A, which is asymmetrical (indium on one surface), polarity should have an effect; but no variation in M was noted.

III. THEORY OF THE MULTIPLICATION EFFECT

A. INTRODUCTION

In the Interim Technical Report (ITR) we presented an initial theoretical analysis based on a one-dimensional model. Charge carriers were assumed to be generated at the surface of the photoconductor by a light beam whose coefficient of absorption was essentially infinite. The carrier was then allowed to diffuse into the photoconductor, allowance being made for recombination (with recombination centers) and ambipolar diffusion. This picture was chosen in view of the experimental results which showed that the multiplication factor does not vary with the angle of the incident beam (ITR, p. 42 ff), which could be interpreted to mean that all charge carriers are generated in the immediate vicinity of the surface.

The expression for the charge carrier concentration, c, thus obtained is an exponential:

$$c = e^{-px}$$

$$-p = \frac{\mu E}{2D} \left(1 - \sqrt{1 + \frac{4kD}{\mu^2 E^2}} \right)$$

(k = recombination rate constant; D = diffusion constant;
μ = mobility of charge carriers; E = applied electric field)

At high fields ($\mu^2 E^2 >> 4kD$) this reduces to

$$p = \frac{k}{\mu E}$$

It can be shown that this approach does not account for the very striking wavelength dependence of M. On the other hand, it can, in principle, account for the electric field dependence.

A second approach is that originally used by I. Bleicher of General Precision when the effect was first discovered in 1963. The charge carriers are assumed to be generated by the Beer-Lambert absorption of light throughout the bulk of the photoconductor and to be essentially immobile thereafter, so that we have

$$c = e^{-\alpha x}$$

where α (cm^{-1}) is the absorption coefficient of the impinging light. Since α varies with wavelength, this model can, in principle, explain the effect of wavelength, but it is incapable of describing the effect of varying the applied field on M.

Since both models give exponential expressions for c, they give essentially similar expressions for the multiplication factor. These have the form

$$M = P \frac{\sinh Q}{\arctan R - \operatorname{arccot} R}$$

Since we have observed that both wavelength and field influence the value of M, we are led to attempt a description which will combine features of both models. This model will provide for both the deposition of charge carriers throughout the photoconductor by the light that penetrates it and their subsequent diffusion and recombination. Both field and wavelength dependence will thus be built into it.

It is of course necessary to reconcile this approach with our results showing no dependence of M on angle of illumination. Three considerations help us to do this, at least qualitatively:

1) The commercial photoconductors used for these experiments were quite thin (50-75μ), so that even slanted beams would produce but little displacement of the charge carriers. In fact, the diameter of the spots exceeds the photoconductor thickness.

2) The angles of illumination deviated by no more than 27.5° from the normal.

3) In view of the high index of refraction of CdS (2.5), the path of the light rays inside the photoconductor was deviated toward the normal.

It should be noted that if this or any other purely mathematical model gives a good representation of the multiplication effect without recourse to specific material properties, it would follow that the multiplication phenomenon would be general to all photoconductors.

B. NEW MATHEMATICAL MODEL

As stated earlier, one main problem in any model is to obtain an explicit expression for $c(x)$. We can write a differential equation for the steady state concentration ($\frac{\partial c}{\partial t} = 0$):

$$D \frac{d^2c}{dx^2} - \mu E \frac{dc}{dx} - kc + \alpha I e^{-\alpha x} = 0$$

Here the first term represents the diffusion of the charge carriers, the second their motion in the field, the third their recombination, as in ITR, p. 55. The fourth term is a source function which represents the generation of charge carriers by incoming light which is attenuated exponentially (with absorption coefficient α cm^{-1}) as it passes through the photoconductor. The quantity I has dimensions of charge carriers per cm^2 per sec and is proportional to the light intensity, which is thus also brought into the model.

This equation can be written

$$\left(\frac{d^2}{dx^2} + a_1 \frac{d}{dx} + a_2 \right) c = f(x)$$

where $a_1 = -\mu E/D$, $a_2 = k/D$, $f(x) = -\frac{\alpha I}{D} e^{-\alpha x}$

The left hand term can be separated into two factors:

$$\left(\frac{d}{dx} - r_1\right)\left(\frac{d}{dx} - r_2\right) c = f(x)$$

where

$$r_1 = \frac{\mu E}{2D} \left(1 + \sqrt{1 + \frac{4kD}{\mu^2 E^2}} \right)$$

$$r_2 = \frac{\mu E}{2D} \left(1 - \sqrt{1 + \frac{4kD}{\mu^2 E^2}} \right)$$

Note that r_1, r_2 are identical with the factors used for solution of the differential equation in the ITR, p. 55; it is therefore expected that the solutions will be related.

We now introduce the new variable

$$\left(\frac{d}{dx} - r_2 \right) c = u$$

The new equation is

$$\frac{du}{dx} - r_1 u = f(x)$$

This is a linear equation whose solution is:

$$u = e^{r_1 x} \int e^{-r_1 x} f(x)\, dx + c'_1 e^{r_1 x} = e^{r_1 x} \left[\varphi(x) + c'_1 \right]$$

where

$$\varphi(x) = \int e^{-r_1 x} f(x) dx$$

From the definition of u:

$$\frac{dc}{dx} - r_2 c = e^{r_1 x} \left[\varphi(x) + c'_1 \right],$$

This is another linear equation which has the solution

$$c = e^{r_2 x} \int e^{(r_1 - r_2)x} \left[\varphi(x) + c_1 \right] dx + c_2 e^{r_2 x}$$

$$= e^{r_2 x} \int e^{(r_1 - r_2)x} \varphi(x) dx + c_1 e^{r_1 x} + c_2 e^{r_2 x},$$

where

$$c_1 = \frac{c'_1}{r_1 - r_2}$$

In this solution, the last two terms are identical with the solution of the homogeneous equation (ITR, p. 55) which lacks the source function. The first term is known as the particular integral of the equation.

We now substitute and first evaluate $\varphi(x)$:

$$\varphi(x) = - \int e^{-\frac{\mu E x}{2D}\left(1 + \sqrt{1 + \frac{4kD}{\mu^2 E^2}}\right)} \frac{\alpha I}{D} e^{-\varphi x} \, dx$$

$$= \frac{\frac{\alpha I}{D} e^{-\left[\alpha + \frac{\mu E}{2D}\left(1 + \sqrt{1 + \frac{4kD}{\mu^2 E^2}}\right)\right] x}}{\alpha + \frac{\mu E}{2D}\left(1 + \sqrt{1 + \frac{4kD}{\mu^2 E^2}}\right)}$$

From this we obtain:

$$c(x) = e^{\frac{\mu E x}{2D}\left(1 - \sqrt{1 + \frac{4kD}{\mu^2 E^2}}\right)} \int e^{\frac{\mu E x}{D}\sqrt{1 + \frac{4kD}{\mu^2 E^2}}}$$

$$\cdot \frac{\frac{\alpha I}{D} e^{-\left[\alpha + \frac{\mu E}{2D}\left(1 + \sqrt{1 + \frac{4kD}{\mu^2 E^2}}\right)\right] x}}{\alpha + \frac{\mu E}{2D}\left(1 + \sqrt{1 + \frac{4kD}{\mu^2 E^2}}\right)} \, dx$$

$$+ c_1 e^{\frac{\mu E x}{2D}\left(1 + \sqrt{1 + \frac{4kD}{\mu^2 E^2}}\right)} + c_2 e^{\frac{\mu E x}{2D}\left(1 - \sqrt{1 + \frac{4kD}{\mu^2 E^2}}\right)}$$

$$= \frac{\frac{\alpha I}{D} e^{-\alpha x}}{\left[\alpha + \frac{\mu E}{2D}\left(1 + \sqrt{1 + \frac{4kD}{\mu^2 E^2}}\right)\right]\left[\alpha + \frac{\mu E}{2D}\left(1 - \sqrt{1 + \frac{4kD}{\mu^2 E^2}}\right)\right]}$$

$$+ c_1 e^{\frac{\mu Ex}{2D}\left(1+\sqrt{1+\frac{4kD}{\mu^2E^2}}\right)} + c_2 e^{\frac{\mu Ex}{2D}\left(1-\sqrt{1+\frac{4kD}{\mu^2E^2}}\right)}$$

$$= \frac{-\alpha I e^{-\alpha x}}{\alpha^2 D + \alpha\mu E - k} + c_1 e^{\frac{\mu Ex}{2D}\left(1+\sqrt{1+\frac{4kD}{\mu^2E^2}}\right)} + c_2 e^{\frac{\mu Ex}{2D}\left(1-\sqrt{1+\frac{4kD}{\mu^2E^2}}\right)}$$

which is the general solution of our differential equation.

We now introduce boundary conditions to obtain a specific solution. The first condition is $c(\infty) = 0$, which requires $c_1 = 0$. The second condition is not so obvious. One possibility is to fix the concentration of charge carriers at the illuminated surface, $c(0) = c_o$

$$\frac{-\alpha I}{\alpha^2 D + \alpha\mu E - k} + c_2 = c_o$$

$$c = \frac{-\alpha I e^{-\alpha x}}{\alpha^2 D + \alpha\mu E - k} + \left(c_o + \frac{\alpha I}{\alpha^2 D + \alpha\mu E - k}\right) e^{\frac{\mu Ex}{2D}\left(1-\sqrt{1+\frac{4kD}{\mu^2E^2}}\right)}$$

For illumination from the other side, the differential equation is

$$D\frac{d^2c'}{dx^2} - \mu E\frac{dc'}{dx} - kc' + \alpha' I' e^{-\alpha(d-x)} = 0 \quad \text{(d - thickness of photoconductor)}$$

which differs only in the source function $f(x)$.

We can then write

$$\varphi'(x) = -\int e^{-\frac{\mu Ex}{2D}\left(1+\sqrt{1+\frac{4kD}{\mu^2E^2}}\right)} \frac{\alpha' I'}{D} e^{-\alpha'(d-x)} dx$$

$$= \frac{\alpha' I'}{D} \frac{e^{-\frac{\mu Ex}{+2D}\left(1+\sqrt{1+\frac{4kD}{\mu^2E^2}}\right) - \alpha'(d-x)}}{\frac{\mu E}{2D}\left(1+\sqrt{1+\frac{4kD}{\mu^2E^2}}\right)^{-\alpha'}}$$

$$c'(x) = e^{\frac{\mu Ex}{2D}\left(1-\sqrt{1+\frac{4kD}{\mu^2E^2}}\right)} \int e^{\frac{\mu Ex}{D}\sqrt{1+\frac{4kD}{\mu^2E^2}}} \frac{\frac{\alpha' I'}{D} e^{-\alpha'(d-x) - \left(1+\sqrt{1+\frac{4kD}{\mu^2E^2}}\right)\frac{\mu Ex}{2D}}}{\frac{\mu E}{2D}\left(1+\sqrt{1+\frac{4kD}{\mu^2E^2}}\right) - \alpha'} dx$$

$$+ c_1 e^{\frac{\mu Ex}{2D}\left(1+\sqrt{\frac{4kD}{\mu^2E^2}}\right)} + c_2 e^{\mu Ex\left(1-\sqrt{1+\frac{4kD}{\mu^2\ E^2}}\right)}$$

$$= \frac{-\alpha' I' e^{-\alpha'(d-x)}}{\alpha'^2 D - \alpha'\mu E - k} + c_1 e^{\frac{\mu Ex}{2D}\left(1+\sqrt{1+\frac{4kD}{\mu^2E^2}}\right)} + c_2 e^{\frac{\mu Ex}{2D}\left(1\sqrt{1+\frac{4kD}{\mu^2E^2}}\right)}$$

The first boundary condition now is $c(-\infty) = 0$, giving $c_2 = 0$

The second is $c'(d) = c_o'$, giving

$$c' = \frac{-\alpha I' e^{-\alpha'(d-x)}}{\alpha'^2 D - \alpha'\mu E - k} + \left(c_o' + \frac{\alpha I}{\alpha'^2 D - \alpha'\mu E - k}\right) e^{\frac{-\mu E(d-x)}{2D}\left(1-\sqrt{1+\frac{4kD}{\mu^2E^2}}\right)}$$

The photocurrents are given by $i_1 = \dfrac{V}{R} = \dfrac{V}{\int_o^d dR} = \dfrac{V}{\int_o^d \frac{m dx}{c}}$

$i_2 = \dfrac{V}{\int_o^d \frac{m dx}{c'}}$, $i_T = \dfrac{V}{\int_o^d \frac{m dx}{c+c'}}$, where V is the applied voltage, R the resistance, and m a proportionality factor which cancels out when we calculate the multiplication factor M;

$$M = \frac{i_T}{i_1 + i_2}$$

$$M = \frac{\left[\int_0^d (c + c')^{-1}\, dx\right]^{-1}}{\left(\int_0^d c^{-1}\, dx\right)^{-1} + \left(\int_0^d c'^{-1}\, dx\right)^{-1}}$$

We wish to point out that this equation contains an approximation in that the field E is taken as a constant, whereas it really varies with depth, the voltage drop being greatest where the resistance is greatest. However, it is assumed that the equation is good enough to justify further work.

The integral

$$I = \int_0^d \frac{dx}{c} = \int_0^d \frac{dx}{Ae^{-\alpha x} + Be^{-\beta x}}$$

can be transformed by the substitution $y = A + Be^{(\alpha - \beta)x}$

$$I = \frac{B^{-\beta/\alpha}}{\alpha - \beta} \int_{A + B}^{A + Be^{(\alpha - \beta)d}} \frac{(y - A)^{\frac{\beta}{\alpha - \beta}}\, dy}{y}$$

This expression is still not integrable in closed form. However, the term:

$$(y - A)^{\beta/(\alpha - \beta)}$$

can be expanded binomially. Each term can then be divided by y and integrated.

An infinite series results, which has no general convergence or sum. The special cases in which α/β is an integer do have sums. Here α is the absorption coefficient and

$$\beta = \frac{\mu E}{2D} \left(1 - \sqrt{1 - \frac{4kD}{\mu^2 E^2}} \right),$$

so that there is no reason to expect α/β to be integral. The summation will thus be a computer problem in most cases. Moreover, the integration

$$dx/(c + c') = \quad dx/(Ae^{-\alpha x} + Be^{-\beta x} + A'e^{-\alpha' x} + B'e^{-\beta' x})$$

has not been brought even to this point. Thus, there is no advantage to this procedure as compared to direct numerical integration.

It was concluded that closed-form integration was impractical and that numerical integration was required. A program was therefore written for the IBM 7040 computer at the General Precision Data Processing Center. This is a relatively simple FORTRAN program which gives the multiplication factor directly.

C. COMPUTATION OF THE MULTIPLICATION FACTOR

1. Early Results

Our first concern was to compute large values of M, i.e., M values greater than 10. It should be stressed that our model gives M as a function of ten independent parameters, and it is therefore not practical to attempt to compute M for all possible sets of conditions (i.e. parameter values) unless something is known about the range of parameter values.

Table 12 shows the results of the first runs. The parameter values and the resulting multiplication factor are shown. The values of k (recombination constant) and d (cell thickness) were not changed and are given at the head of the table. Where other values are blank, they are the same as the next value printed above. Parameter values were selected to conform to actual values when known; but some values are not known even approximately.

It will be seen that initial attempts gave values of M very near to unity. (However, no value below unity was obtained; such a result would indicate an error in the model). The effect of varying the values of α (and α') and of μE was then sought. It was found that M is more sensitive to μE than to α. As μE is increased, M goes through a maximum (μE = 10,000, M = 1.2) and then drops again. At a given value of μE, the effect of changing α is very slight.

TABLE 12

Calculated Values of Multiplication Factor

k=100, d=0.005

D	μ E	I	I'	c_o	c_o'	α	α'	M
0.1	2.0	1×10^{-1}	2×10^{-1}	1×10^{-2}	2×10^{-2}	500	1000	1.00070
		1×10	2×10	1×10^{0}	2×10^{0}			1.00070
		1×10^{5}	2×10^{5}	1×10^{4}	2×10^{4}			1.00070
		1×10^{7}	2×10^{7}	1×10^{6}	2×10^{6}			1.00070
		1×10^{9}	2×10^{9}	1×10^{8}	2×10^{8}			1.00070
		1×10^{11}	2×10^{11}	1×10^{10}	2×10^{10}			1.00070
		1×10^{13}	2×10^{13}	1×10^{12}	2×10^{12}			1.00070
		1×10^{15}	2×10^{15}	1×10^{14}	2×10^{14}			1.00070
10.0	200	1×10^{13}	2×10^{13}	1×10^{12}	2×10^{12}	500	1000	1.00020
							5000	1.00020
	2,000						1000	1.02052
							5000	1.02055
	10,000						1000	1.19658
							5000	1.19660
	20,000						1000	1.12300
							5000	1.12294
	30,000						5000	1.07962
	40,000						5000	1.05875
	80,000						5000	1.02889
10.0	10,000					1000	1000	1.19600
						2000		1.19604
						4000		1.19606
						8000		1.19608
						1000		1.12242
	20,000					2000		1.12244
						4000		1.12244
						8000		1.12245

Some of these values were computed by hand to verify that the computer program was free of errors. These values seem to indicate that while (as stated previously) this model implies that the current multiplication effect is a property of all photoconductors, there may be large regions in which it is not perceptible, i.e. M is very near unity.

Further runs with different sets of parameters yielded M values no higher than $M = 1.5$. In view of the apparent difficulty in obtaining M values much greater than 1, it was necessary to define our objectives, and criteria of success of the model. The model would be considered satisfactory to the extent that the following conditions were met.

a. Values of the multiplication factor M as large as those observed can be computed.

b. The experimentally observed parameter dependences can be computed, and the results of new experiments predicted.

c. The existence (or nonexistence) of a multiplication effect can be predicted in other photoconductors and verified by experiment.

2. ONESTEP Program

A review of the inherent problems in computing large values of M, led to the conclusion that more efficient computer programs had to be used. Some simple changes in the original program allowed approximately a forty-fold decrease in IBM 7040 computer time. However, substantial improvements in analysis and programming time were sought.

To this end, the existing computer program was modified to produce the ONESTEP version. In this version, the value of one of the parameters is varied stepwise for a predetermined number N of steps. Therefore, for a single set of input parameter values, N values of the multiplication factor are computed, where N can be as large as 1000.

Using the ONESTEP program to vary the parameters c_o, μE, and D -- each one over a wide range of values -- a set of parameter values was found which gave $M = 5.73$. This set is:

D	=	10	α	=	500	α'	=	10^3
μE	=	1.7×10^4	l	=	10^{13}	l'	=	2×10^3
k	=	100	c_o	=	1	c_o'	=	2×10^{12}

(All values in cgs units).

3. SEARCH program

Another program - SEARCH - was written which varies all of the parameters stepwise, and sequentially, in a predetermined sequence. In this program, starting with a single input set of parameters, automatic variations in the parameters lead to ever increasing values of M. Feedback is built into the program to ensure that the variation of each parameter in turn continues only while M is increasing. Thus the program seeks out a maximum value of M.

The ONESTEP program was designed primarily to find suitable starting points in the ten-dimensional parameter space for the SEARCH program. However, the rapid success of the SEARCH program eliminated the need for ONESTEP.

After debugging, the SEARCH program immediately yielded a large value of the multiplication factor ($M = 2.0 \times 10^{10}$). Inspection showed that this was not a maximum but rather a boundary of the region which the computer handles (it is incapable of handling very large numbers, e.g., e^x for $x > 88$). Several other runs also gave similar results.

Some of the results of the SEARCH runs are given in Table 13. The first line shows the "standard" set of conditions and the second shows the highest previously attained value of M. The third line shows the highest value obtained with ONESTEP before SEARCH was used. These first three lines are included for comparison. The next 12 lines show the results of three SEARCH runs. In each case, the values of the parameters are shown for the M values nearest 10,000 and 1000 and for the maximum value of M. The three SEARCH runs differ only in stepping order (of the parameters) and/or the stepping factor.

TABLE 13

Parameter Values

	D	μE	k	α	I	c_o	α'	I'	c_o'	d	M
1. Standard Set	10	10^4	10^2	500	10^{13}	10^{12}	10^3	2×10^{13}	2×10^{12}	5×10^{-3}	1.196
2. Largest M prior to ONESTEP	9	"	"	"	"	10^{11}	"	"	"	"	1.499
3. Largest M prior to SEARCH	10	1.7×10^4	"	"	"	1	"	"	"	"	5.730
4. SEARCH Run 4	"	10^4	2.0×10^7	"	"	10^{12}	7.4×10^3	"	2.0×10^{13}	"	10.0
5. " "	"	"	6.2×10^7	"	"	"	"	"	"	"	1.17×10^2
6. " "	"	"	1.1×10^8	2.2×10^6	"	"	"	"	2.2×10^{13}	"	1.02×10^3
7. " "	"	"	9.9×10^8	"	1.1×10^{13}	2.6×10^{12}	1.9×10^4	2.2×10^{13}	3.1×10^{14}	"	1.97×10^{10}
8. " "5	"	"	2.9×10^7	3.3×10^5	10^{13}	10^{12}	10^{13}	2×10^{13}	2×10^{12}	"	10.1
9. " "	"	"	8.3×10^7	"	"	"	"	"	"	"	1.27×10^2
10. " "	"	"	1.2×10^8	"	"	"	3.5×10^3	6.6×10^{16}	"	"	1.00×10^3
11. " "	"	1.1×10^4	9.9×10^8	"	1.2×10^{13}	1.8×10^{12}	1.3×10^4	7.0×10^{18}	1.8×10^{14}	"	1.96×10^{10}
12. " "6	3.9	1.0×10^4	8.6×10^6	5.0×10^2	1.2×10^6	1.8×10^8	1.9×10^3	7.1×10^6	2.0×10^{12}	"	10.5
13. " "	"	"	2.7×10^7	"	"	"	"	"	"	"	1.28×10^2
14. " "	"	"	5.2×10^7	"	"	"	"	"	"	"	1.39×10^3
15. " "	"	"	2.8×10^8	9.6×10^3	1.4×10^6	"	9.1×10^3	"	3.8×10^{13}	"	4.87×10^8

It is seen that the high values of M correspond to large values of k, the recombination rate constant. Two other SEARCH runs gave the same apparent correlation of M with k. In run number 9, a different starting point was chosen, and in addition the parameter k was constrained to have the value k = 100 throughout the run. It was hoped that, in this way, large values of M could be found in a region where k is not large. However, in this run the highest M value was only M = 2.

4. Parameter Dependences. ALLSTEP Program

Having found regions of the parameter space having large M values we desired to compute the dependence of M on each of the parameters at selected points in the high M regions. Initially, ONESTEP was used for these dependence computations. However, since the ONESTEP program is inefficient for this task, another program has been written - ALLSTEP which can compute dependencies for all ten parameters with just a single input.

a. A given set of parameter values is input. These are called the original values (OVs). The OVs define the original point.

b. The ith parameter is changed to a preselected lowest value while the others are kept at their OVs. M is calculated.

c. The ith parameter is then stepped, i.e., multiplied by a small stepping factor. M is again calculated.

d. This process is repeated for a predetermined number of steps. In the process, the ith parameter is increased above its OV. A curve of M versus this parameter is then obtained, with all the other parameters at their OVs.

e. At the end of this process, the ith parameter reverts to its OV and the process is repeated with another parameter.

f. The output is a series of ten sets of M values showing the variation of M with each parameter along a line which includes the OV.

Three ALLSTEP runs have been made. The OVs were the same in all the runs with the exception of the parameter α', as shown in Table 14. The stepping factor was 1.1 and the number of steps was 40. The lowest value of each parameter was one-tenth of the OV. Accordingly, the final value was 4.526 times the OV.

In Table 15, the variations of M as a function of each parameter are shown for the three runs. These data are plotted in Figure 10. It will be seen that the curves are fairly similar in the three runs, with some exceptions (I',d). They constitute an interesting description of the multi-dimensional M surface by means of its cross sections. These particular dependences do not correspond precisely with any experimental results, which indicates that the original values do not correctly represent the conditions of our experiments.

D. INTERPRETATION

From these results the following conclusions have been drawn.

It has been demonstrated that the mathematical model can yield values of M as high as, and higher than, any experimental values. It now remains to be seen whether realistic parameter dependencies can be obtained.

Apparently the large values of M are found in a region in which M is strongly dependent on the recombination rate constant k.

This variation can, perhaps, be rationalized. There are three characteristic times which can be obtained from the parameters:

1. The time needed for an electron to diffuse across the cell, which is roughly $d^2/4D$;
2. The time needed for an electron to be pulled across the cell by the applied field, which is $d/\mu E$;
3. The lifetime of the electron with respect to recombination, which is $1/k$.

These characteristic times are shown in Table 16.

TABLE 14

VALUES OF PARAMETERS AND M AT PRESELECTED POINTS OF ALLSTEP PROGRAM

1. Diffusion Constant D		$10\ cm^2/sec$
2. Field Strength x Mobility μE		1000 cm/sec
3. Recombination Constant k		$1.1 \times .0^8\ sec^{-1}$
4. Absorption Coefficient (left) α		$500\ cm^{-1}$
5. Intensity (left) I		$1 \times 10^{13}\ cm^{-2}\ sec^{-1}$
6. Surface Concentration (left) c_o		$1 \times 10^{12}\ cm^{-3}$
7. Absorption Coefficient (right) α':		
	Run 1	$7400\ cm^{-1}$
	Run 2	$740\ cm^{-1}$
	Run 3	$74\ cm^{-1}$
8. Intensity (right) I'		$2 \times 10^{13}\ cm^{-2}\ sec^{-1}$
9. Surface Concentration (right) c'_o		$1.97 \times 10^{13}\ cm^{-3}$
10. Cell Thickness		5×10^{-3} cm

Values of M at preselected point:

Run 1	319.25
Run 2	185.30
Run 3	132.94

FIGURE 10

THEORETICAL PARAMETER DEPENDENCES ALLSTEP RUNS 1, 2, AND 3. (See Table)

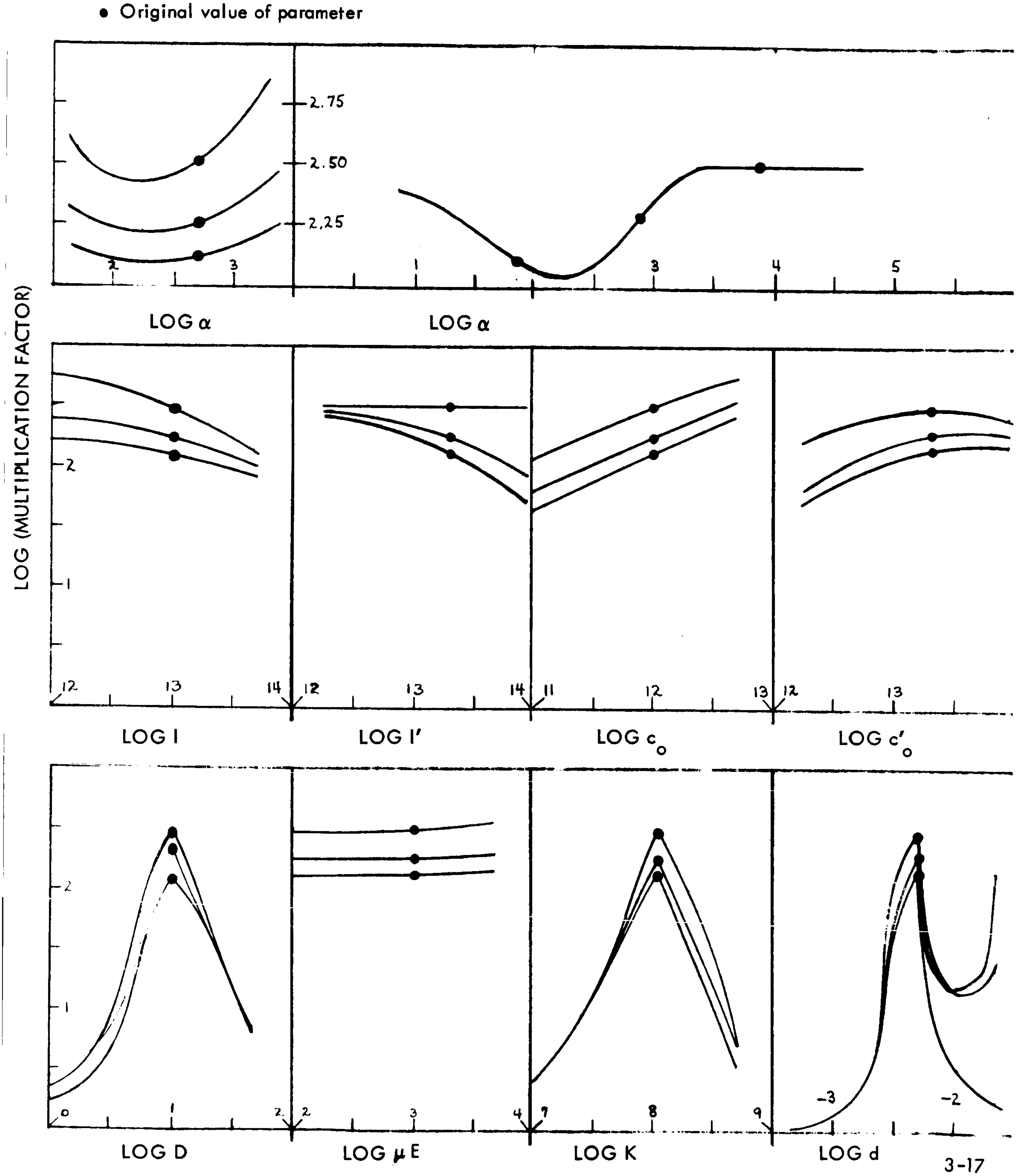

TABLE 15

VALUES OF M ALONG CROSS-SECTION THROUGH THE ORIGINAL POINTS (ALLSTEP PROGRAM)

1. Diffusion Constant. Sharp peak near preselected value

	D =	1	2.36	5.56	9.85	21.11	45.26 $cm^2 sec^{-1}$
Run 1	M =	2.31	4.68	70.69	321.64	44.56	7.39
Run 2	M =	2.75	4.31	34.02	182.52	44.11	7.39
Run 3	M =	1.83	2.96	24.85	130.28	43.59	7.39

2. Mobility x Field Strength. Very slow rise

	μ E	100	236	556	985	2111	4526 cm sec^{-1}
Run 1	M =	299.16	302.37	309.70	318.94	339.36	359.81
Run 2	M =	178.33	179.45	182.00	185.19	192.28	200.82
Run 3	M =	128.77	129.43	130.95	132.87	137.36	144.05

3. Recombination Constant. Sharp peak near preselected value

	k =	1.1	2.59	6.12	10.84	23.22	49.79 x 10^7 sec^{-1}
Run 1	M =	2.64	9.38	75.74	314.24	67.19	6.18
Run 2	M =	2.64	9.36	72.14	186.06	32.62	5.27
Run 3	M =	2.64	9.34	68.24	134.15	23.89	3.65

4. Absorption Coefficient (left). Shallow minimum

	α =	50	118	278	492	1056	2263cm^{-1}
Run 1	M =	363.20	288.05	266.57	316.75	531.70	655.34
Run 2	M =	198.90	174.23	166.27	184.46	240.74	262.72
Run 3	M =	139.66	127.05	122.82	132.51	159.24	168.43

5. Intensity (left). Slow decrease

	I =	1	2.36	5.56	9.85	21.11	45.26x$10^{12}$$cm^{-2}$$sec^{-1}$
Run 1	M =	572.78	502.71	400.92	321.39	217.32	132.96
Run 2	M =	248.35	234.34	209.80	186.01	146.05	102.80
Run 3	M =	162.36	156.28	145.02	133.30	111.56	84.57

Table 15 (cont'd)

6. Surface Concentration (left). Increase, approximately as 0.5 power of parameter

	c_o =	1	2.36	5.56	9.85	21.11	45.26×10^{11} cm^{-3}
Run 1	M =	118.14	173.23	250.81	317.32	424.84	547.90
Run 2	M =	64.34	95.97	142.39	184.06	255.75	346.60
Run 3	M =	44.96	67.56	101.24	132.02	186.28	257.94

7. Absorption Coefficient (right) (Combination of three runs) Minimum, then rise to flat shelf

α' =	7.4	17.4	37.4	74.0	174	374 cm^{-1}
M =	253.57	209.38	166.29	132.94	108.79	118.09
α' =	740	1745	3740	7289	15624	33492 cm^{-1}
M =	185.30	312.71	319.25	319.25	319.25	319.25

8. Intensity (right). Flat (Run 1); slow decrease (Runs 2 and 3)

	I' =	2	4.72	11.12	19.70	42.23	90.52×10^{12} cm^{-2} sec^{-1}
Run 1	M =	319.25	319.25	319.25	319.25	319.25	319.25
Run 2	M =	293.81	267.08	223.45	186.34	133.75	86.97
Run 3	M =	267.34	225.40	171.36	133.90	89.31	55.35

9. Surface Concentration (right). Flat maximum (Runs 1 and 2); slow increase (Run 3)

	c_o' =	1.97	4.65	10.95	19.40	41.59	89.16×10^{12} cm^{-3}
Run 1	M =	173.23	239.00	298.72	319.03	307.80	260.15
Run 2	M =	91.66	125.20	162.50	184.79	202.12	196.71
Run 3	M =	68.27	90.86	116.21	132.54	149.16	153.92

10. Cell thickness. Sharp maximum at preselected point; then minimum (Runs 1 and 2), sharp descent (Run 3)

	d =	5	11.8	27.8	49.2	105.6	226.3×10^{-4} cm
Run 1	M =	1.05	1.54	15.4	307.98	14.9	22.49
Run 2	M =	1.05	1.54	15.3	184.87	16.21	112.47
Run 3	M =	1.05	1.54	15.4	136.61	3.35	1.82

TABLE 16

CHARACTERISTIC CARRIER LIFETIMES

	M	$d^2/4D$ (sec)	$d/\mu E$ (sec)	$1/k$ (sec)
1. Standard Set	1.196	6×10^{-7}	5×10^{-7}	1×10^{-2}
2. Largest M prior to ONESTEP	1.499	7×10^{-7}	"	"
3. Largest M prior to SEARCH	5.730	6×10^{-7}	3×10^{-7}	"
4. SEARCH Run 4	10.0	"	5×10^{-7}	5×10^{-8}
5. " "	1.17×10^{2}	"	"	2×10^{-8}
6. " "	1.02×10^{3}	"	"	1×10^{-8}
7. " "	1.97×10^{10}	"	"	1×10^{-9}
8. " " 5	10.1	"	"	3×10^{-8}
9. " "	1.27×10^{2}	"	"	1×10^{-8}
10. " "	1.00×10^{3}	"	"	1×10^{-8}
11. " "	1.96×10^{10}	"	"	1×10^{-9}
12. " " 6	10.5	3×10^{-7}	"	1×10^{-7}
13. " "	1.28×10^{2}	"	"	4×10^{-8}
14. " "	1.39×10^{3}	"	"	2×10^{-8}
15. " "	4.87×10^{8}	"	"	3×10^{-9}

It will be recognized that recombination becomes important when the recombination lifetime is equal to or smaller than the other times. A strong dependence on k is then expected.

But it is precisely under such conditions that a maximum multiplication effect can be expected. If k is large, the electron will travel only a short distance before it recombines ($\mu E/k \ll d$). It is effectively localized. Under these conditions, we approximate the original Bleicher model* which allowed for no charge carrier motion at all. Differences in concentration of charge carriers across the cell, caused by large values of α and α', are not blurred and thus the multiplication effect, which could be based on local variation of this concentration, can be very marked. If, on the other hand, k is much smaller than $\mu E/d$ and $4D/d^2$, such concentration inequalities will be smoothed out and only small values of M can be expected.

It should be noted however, that further computations of M in other regions of the parameter space may yet yield large M values at low values of k ($k \approx 100$). In fact, rough calculations indicate that such a region may be found for extremely low values of the diffusion constant D (ca. 10^{-7}) and low values of the mobility μE (ca. 10^{-2}).

The variation of M with the individual parameters is not monotonic. In face, the multidimensional M surface exhibits peaks, ridges, and valleys. Some of these are seen in Table 15 and Figure 10. The experimental data also show peaks and valleys (Figures 1-5) which resemble the calculated ones in general aspect, but by no means correspond in detail. We consider even this general resemblance a hopeful result, and believe that it is worthwhile to continue work on the mathematical model with the aim of matching experimental results more closely.

* See page 3-1.

IV. BREADBOARD BEAM FOLLOWER

The construction and analysis of a breadboard beam follower based on the photoconductive multiplication effect was undertaken in order to demonstrate the potential utility of the phenomenon in space communications and navigation. It was expected that observations made on the breadboard model would permit an analysis to be made which would give quantitative predictions of the properties of devices based on the effect.

Design and construction of the beam follower were largely performed by an engineering team at General Precision's GPL laboratories, in particular by Messrs. R. Flower and C. Olfers, working under the general supervision of Mr. G. Stavis. The general design was fixed by consultation with Research Center personnel (Drs. F. B. Berger, D. Grafstein, R. P. Borkowski, A. H. Samuel) and the selection and mapping of a suitable photocell was performed by Mr. J. C. Scanlon.

The design was fixed in January 1966; the mapped cell was delivered by March 1; and the beam follower was completed and delivered to the Research Center on June 28. After performance measurements and analyses, the beam follower was brought to NASA/ERC, Cambridge, on August 24, installed and demonstrated there. After some consideration of its fate, it was decided that it should be restored to Little Falls and maintained in an operating condition there. It was accordingly returned to Little Falls on November 1 and was in an operating condition as this report was written.

In this section we first describe the beam follower, with particular emphasis on the properties of the photocell. The testing program for the instrument is then described, followed by an analysis of the results and their relevance to possible applications.

A. Design of Breadboard Beam Follower

The breadboard device demonstrates the capability to align automatically two light beams which illuminate opposite sides of the photoconductor cell. To avoid undue complexity, a system having only one degree of freedom was produced. The signal beam source was mounted on a carriage driven by a manually operated lead screw, permitting translation over a distance of 4" in the direction transverse to the beam axis. The bias beam source and photoconductor were mounted on a similar carriage to which a servo drive was applied. The carriages were available at General Precision and were modified to accommodate the necessary drive mechanism. The photoconductor provides an error signal, enabling its servo to drive to a null position as it tracks the signal light source. The null condition occurs when the signal and bias beams are in coincidence on opposite sides of the photoconductor.

Let us consider the (horizontal) direction of the beam as the X direction and the normal horizontal direction as the Y direction. Both modules move on tracks in the Y direction. The beam generator, which can be moved manually, contains a monochromatic light source and lens system to produce a well-defined spot on the surface of the photoconductor of the beam follower. The beam follower contains the photoconductor and its holder, which is coupled to an electrically driven screw, so that it can travel over a 10 centimeter range in the Y direction. The bias beam is generated by a static light source which emits a beam in the Y direction. This is deflected to the X direction by a mirror which travels with the beam follower module. This mirror vibrates to produce the sense direction information required. The photoconductor current is fed into the electronic mechanism which activates the beam follower screw to seek a photocurrent maximum.

As finally built, the breadboard beam follower consists of two physically separated parts: the optical units and the control unit. On the optical unit base (Figure 11) are mounted:

a. the carriage containing the independently movable light source (master unit),

b. the carriage with the beam follower, light source, and mirror galvanometer,

c. the motor driving the beam follower,

d. two transformers for the 6 volt lamps in the two light sources.

The servo units are mounted in the separate control unit.

These units will now be described briefly.

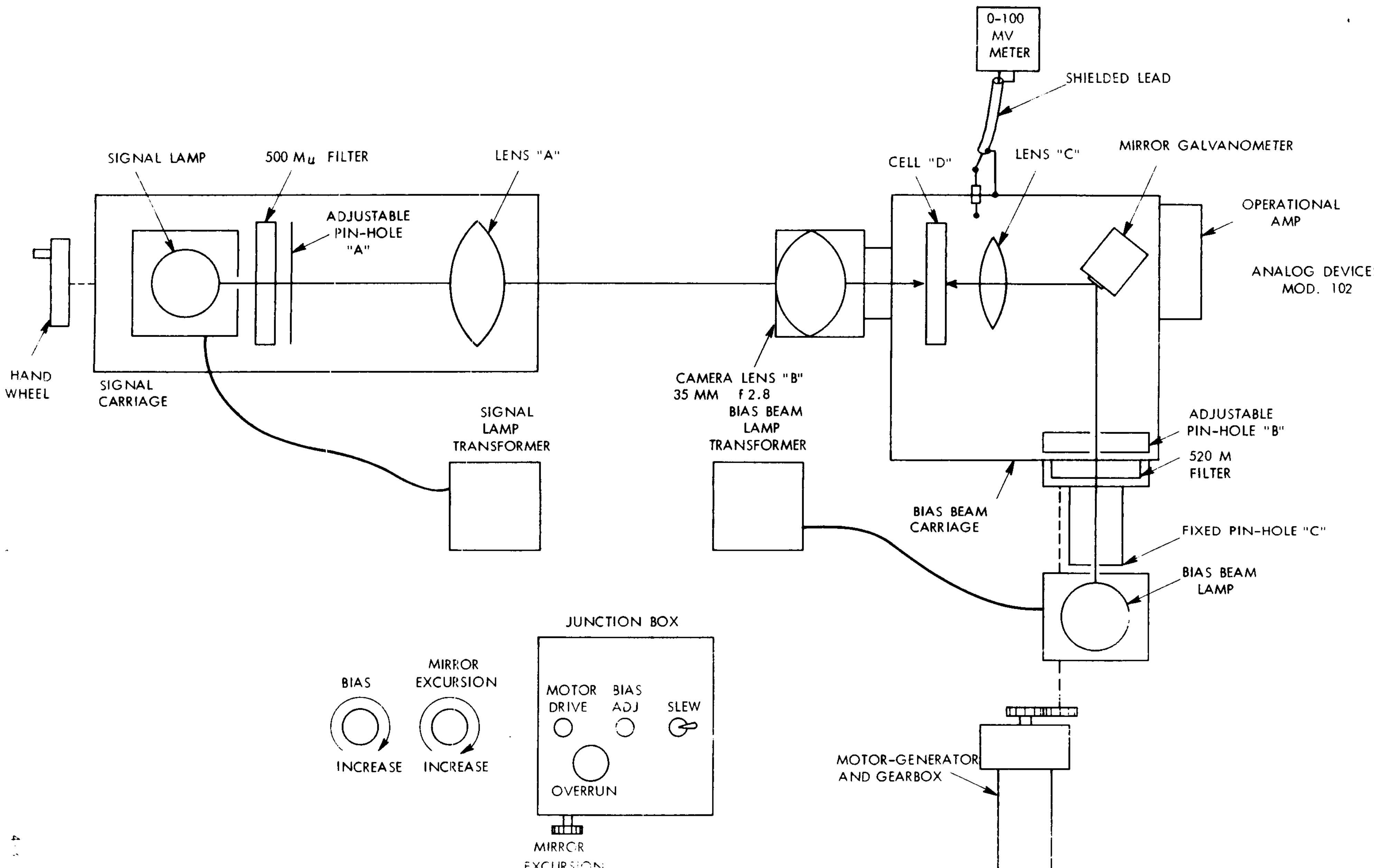

OPTICAL AND MECHANICAL LAYOUT OPTICAL BEAM TRACKER
FIGURE 11

a. The master unit contains a 6 volt auto headlight lamp in a black box. A pinhole, interference filter (5120 Å), and lens produce a nearly parallel, horizontal beam which is directed towards the follower unit. The entire master unit is manually cranked along the carriage.

b. The follower unit contains the photoconductive cell, on which spots are produced from the impinging light beams. The beam from the master unit is focused by a camera lens on the front of the cell; the beam from the 6 volt lamp attached to the follower unit is projected on the back of the cell after passing through an interference filter (5330 A), a lens, and the mirror galvanometer whose null position is at a 45° angle to the X and Y directions. The follower unit is moved along the carriage by the central screw which is driven by the servo motor through a gear. This unit also contains a preamplifier for the photocell signal.

c. The servo motor is attached to the follower carriage and is driven by the error signal emanating from the control unit.

d. The two transformers are fed by AC current which can come directly from the 110 V, 60 cps mains. However, we interposed Variac units for greater control.

e. The control unit has the following function (components underlined):

1. It supplies a 2.0 cps signal to the galvanometer mirror from a <u>2.0 cps timing oscillator</u> and a <u>mirror drive circuit</u>. As a result, the spot falling on the back of the photocell is displaced to either side of the null spot with that frequency. The difference in photocurrent then indicates dM/dY, which is zero when M is maximal, i.e., when the front spot and rear null position coincide. (It is also zero when M = 1 and "tracking has been lost"). This relationship is shown in Figure 4.

2. It accepts the output signal from the preamplifier, amplifies it in a <u>signal voltage</u> amplifier, and compares it in the <u>phase detector</u> with the 2.0 cps reference signal. The difference in current between the two signals determines the polarity and level of the error signal.

FIGURE 4 EFFECT OF LINEAR DISPLACEMENT ON M

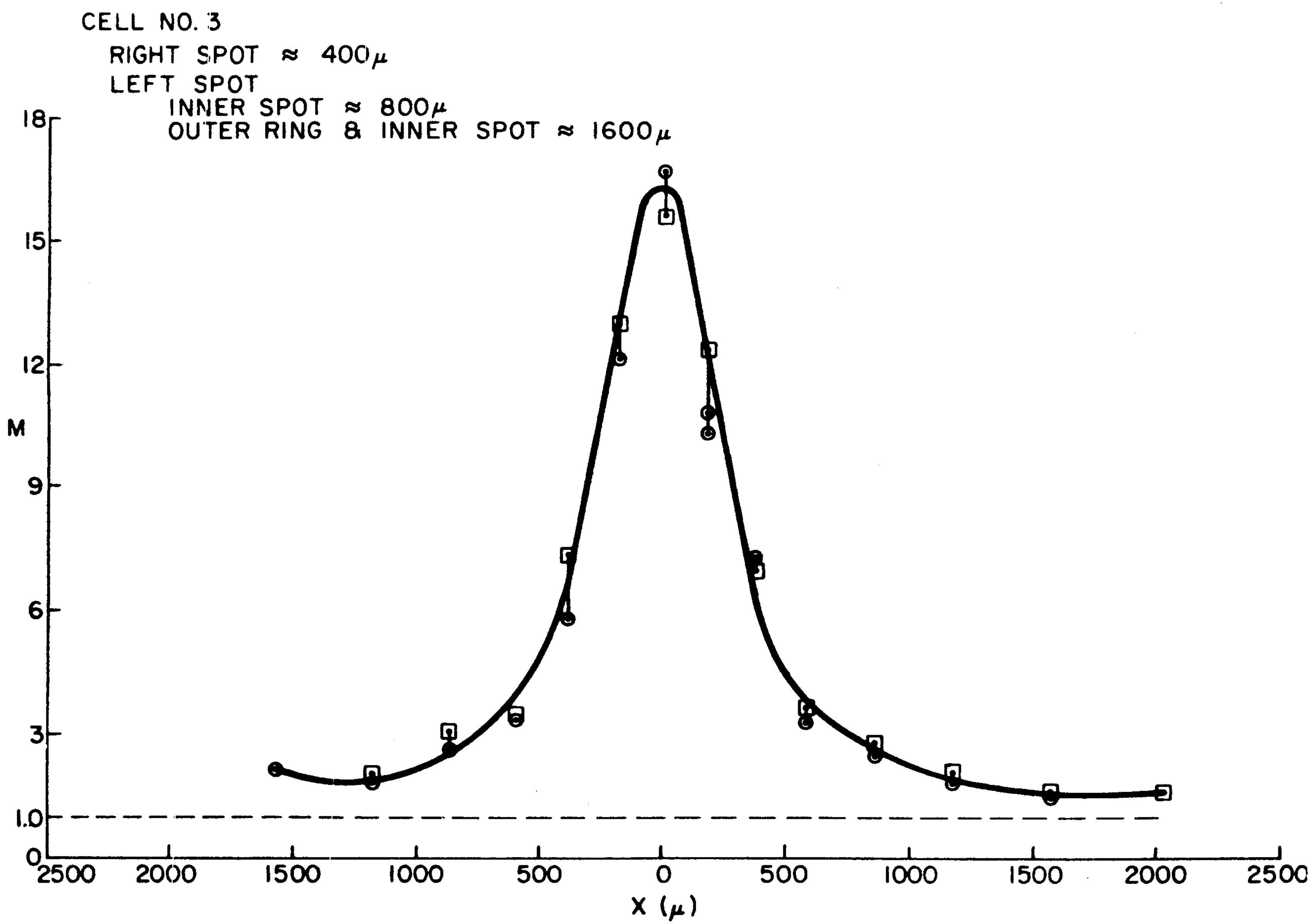

3. It amplifies the error signal in a power amplifier and uses the amplified signal to drive the servo motor. The control also contains power supplies to provide the regulated DC voltages for all circuits in the breadboard unit.

For operation of the breadboard beam follower, the following are required:

a. 115V, 60 cycle AC power.

b. Two Variacs (or equivalent) which take this power and feed the two lamp transformers. By this means, the intensity of the light sources can be regulated.

c. 28V DC power. This serves primarily for the photocell bias.

d. 115V, 400 cycle power, which serves to power the entire servo system.

e. A microvolt-ammeter of suitable input impedance to monitor the current through the photocell and establish whether or not the beam follower is tracking. A Kin-Tel model 203 has been found suitable. However, with a modicum of experience this unit can be dispensed with and the amplitude of the servo signal current can be estimated from the intensity of the noise from the servo motor.

B. Photocell For Breadboard Beam Follower

Before the design parameter of the breadboard beam-following device would be completed and its construction begun, it was necessary that a photoconductive cell with precisely measured characteristics be provided. The first step was the screening of commercial cells for photoconductive sensitivity. This was done by measuring their resistance in the dark and under normal room illumination (fluorescent lights). The resistances were measured by an RCA Senior Voltohmyst both under roomlight conditions (R_L) and in the dark (R_D). Table 17 shows the results.

All the cells of Table 17 showed a change of resistance by at least a factor of 1300. The next step was to check the values of the multiplication factor in these cells. First it was desired to measure this value at different points on the cell, to determine cell uniformity.

TABLE 17

Dark and Light Resistance of Commercial Cells

Cell Designation	R_D (ohms)	R_L (ohms)	R_D/R_L	Comment
B	3.0×10^7	2×10^2	1.5×10^5	Indium Electrode
C	2.4×10^6	80	3×10^4	Indium Electrode
D	2.0×10^5	1.5×10^2	1.3×10^3	Gold Electrode
E	2.0×10^7	9×10^2	2×10^4	Gold Electrode
G	3.0×10^7	1.85×10^4	1.5×10^3	Gold Electrode

Microscope objective - ocular lens combinations were used to obtain spots of light. The diameters of the spots used were no greater than 0.5 mm. Interference filters were employed to isolate the appropriate wavelengths, and neutral density filters were used to modulate the intensity. The photoconductive cell was mounted on an X-Y microscope stage. In this way the multiplication factor could be determined as a function of the position of the spots.

In testing the Cells of Table 17 for uniformity of the multiplication factors, a wavelength combination of 512 and 633 mμ was chosen. The 512 mμ light illuminated the glass electrode and the 633 mμ light illuminated the indium electrode. A bias voltage of 1.0 volt was applied across each photocell, with the indium electrode being negative. A preliminary examination of all five cells indicated that cell D might be most satisfactory. Cell D gave the largest M values and (just as important) these values were uniformly maintained over a larger area of the cell.

For brevity, only the mapping data for cell D are presented in this report.

In Table the multiplication factors at various points of coincidence on photocell D are tabulated. The various abscissas (x), and ordinates (y), correspond to readings taken from the microscope X-Y stage. These points are mapped in Figure 12.

A similar but much more complete mapping of cell D was also accomplished with an applied voltage of 0.5 volts. These data are not given here. They are not essentially different from those of Table 18 .

The mapping operation was continued in an attempt to find a set of wavelengths giving much larger M values. The wavelength combination λ_1 = 533 mμ ; λ_2 = 512 mμ was selected.

This wavelength combination gave much larger M values than any other tried. The photocurrents produced by this combination, however, were lower. The engineers responsible for the construction of the breadboard preferred the largest possible M values to the largest possible currents. Multiplication factors as a function of position for this wavelength combination are presented in Table 19 . A graph of these data indicates that approximately 50% of the active area of the cell gives multiplication factors greater than 100. This area lies in the central position of the photocell. Multiplication factors of 10

TABLE 18

Multiplication Factor as Function of Position

Cell D

V = 1.0 volt

λ_1 = 633 mu + 3.0 neutral density filter (illuminating indium electrode)

λ_2=512 mu (illuminating glass electrode)

Position (x, y) (mm)	i_D	i_1	i_2	i_T	M
	$\times 10^6$ amperes				
A (17.5, 20)	0.02	0.40	0.12	4.0	8.3
B (18.5, 20)	0.06	0.66	0.16	4.8	6.8
C (16.5, 20)	0.08	0.37	0.14	3.8	10.6
D (16.5, 16.5)	0.04	0.19	0.12	2.6	11.1
E (18.5, 16.5)	0.01	0.36	0.04	3.6	9.0
F (16.5, 22.5)	0.04	0.54	0.22	2.2	3.2
G (18.5, 22.5)	0.01	0.52	0.24	2.4	3.1
G (18.5, 22.5)*	0.01	0.54	0.17	4.0	5.8

* After re-alignment of light spots.

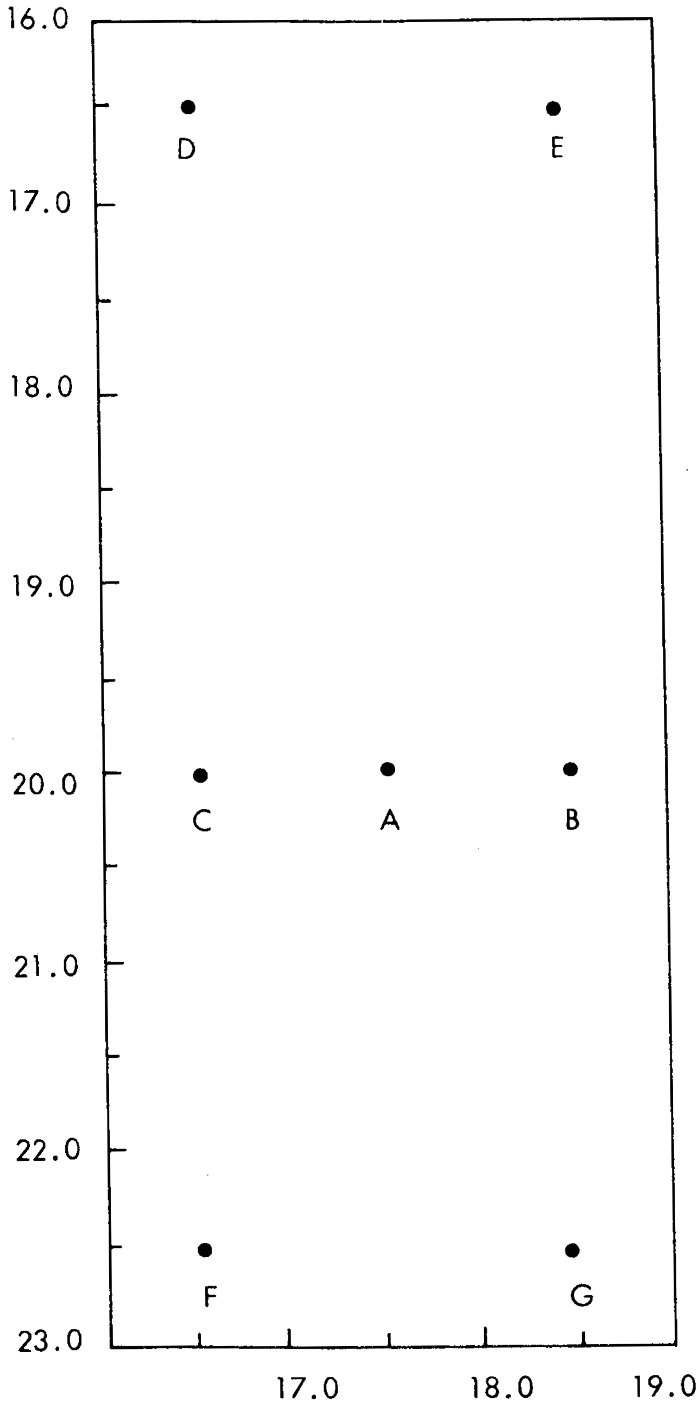

SCALE 1" = 1 MM

MAP OF CELL D

FIGURE 12

TABLE 19

Multiplication Factor As A Function of Position

Cell D
V = 1.0 volt

λ_1 = 533 mμ interference filter + neutral density filter 1.0 + neutral density filter 2.0
(illuminating indium electrode)

λ_2 = 512 mμ interference filter + neutral density filter 3.0 (illuminating glass electrode)

Position (x, y) (mm) x	y	i_1 (amperes x 10^9)	i_2 (amperes x 10^9)	i_T (amperes x 10^9)	M
17	13.5	2.0	1.0	165	55
	17.5	15.0	8.0	430	19
19	11.5	26.0	8.0	530	16
	13.5	~0.0	2.0	300	150
	15.5	1.0	2.0	380	127
	17.5	1.0	0.0	1070	1070
	19.5	1.0	0.0	820	820
21	11.5	2.0	6.0	1030	123
	13.5	8.0	~0.0	690	86
	15.5	3.0	5.0	830	104
	17.5	3.0	1.0	1120	280
	19.5	17.0	~0.0	2100	123
23	13.5	44.0	2.0	250	5
	15.5	10.0	4.0	280	20
	17.5	11.5	10.0	920	7

or greater can be obtained over approximately 90% of the active area of the cell. Multiplication factors less than 10 are found near the edges of the active area.

A notable result of this mapping was the recording, at one spot, of a multiplication factor of 1070, nearly ten times as high as the highest value previously recorded.

This photocell is the one which was used in the breadboard beam follower.

C. Performance Tests

After the beam follower breadboard model was assembled and successfully operated, a number of performance tests were performed.

The following parameters were determined experimentally:

a. Tracking speed

When the master unit of the beam follower is moved too fast, tracking is lost. It is therefore meaningful to establish the maximum tracking rate of the unit. Since the master and follower unit move in parallel, the maximum displacement rate (without tracking loss) is the same for both. The actual displacement rate of the light spot on the photoconductor surface is obtained by multiplying the carriage displacement rate by the distance ratio:

(lens to cell)/(lamp to lens)

In the beam follower this ratio is 1:6.

A panel of three experimentalists was selected to acquire skill in moving the master unit as rapidly as possible without tracking loss. A 5-cm course was selected and it was noted that the time needed to cover this course decreased as experience increased. Eventually, minimum times were obtained as follows:

Direction 1 (increasing number on scale):	40.0 sec.
Direction 2	39.5 sec.

It is concluded that the maximum tracking speed is at least 0.125 cm/sec. The corresponding velocity of the image on the cell is 0.02 cm/sec (0.002 radians/sec).

b. Tracking reproducibility

Millimeter scales with verniers are attached to the carriages of both the master and the follower units. The difference in reading between the two units has a "constant" and a random component. The "constant" component is set during the initial alignment procedure. It can be changed by adjusting the lenses of the optical system so as to change the imaging geometry of the two light spots, but does not vary between adjustments. It has only trivial importance. The random component includes random error of the beam follower device. It also includes random error in positioning the master unit and (if different positions are compared) inequalities of the two scales.

Table 20 shows the results of an experiment designed to measure the random error. The master unit was set at a position and the position of the follower was read after 10 seconds had elapsed. The first part of the table shows the readings when different master positions were set in the order indicated. The second part shows the readings when the same position was approached alternately in either direction. The indicated errors are one standard deviation.

Since the nominal precision of reading and positioning was only 0.1 mm, the standard error of 0.07 to 0.08 mm obtained by this procedure would be a reasonable estimate of the master positioning error alone. It is therefore definitely an upper limit for the inherent error of the beam follower, which may actually be considerably lower.

c. Power requirement

In order to measure the power requirement of the beam follower under normal tracking conditions, the incident light beam was allowed to impinge on a calibrated Eppley bolometer. No deflection was observed, so that it was necessary to remove the interference filter (512 $m\mu$). When this was done, it was found that the light spot induced a deflection of 6.4 ± 2.2 microvolts above background. The entire beam was contained in the sensitive area of the bolometer. The bolometer was calibrated to yield 0.058 microvolts per microwatt. From the absorption spectrum of the interference filter and the color temperature of the lamp (2840° K), it was determined that 0.066 percent of the lamp was passed by the filter. The operating light flux was therefore:

TABLE 20

Beam Follower Error

a.

Master Position (cm)	Follower Position (cm)	Direction
12.00	12.07	2
11.00	11.07	2
10.00	10.07	2
11.00	11.05	1
12.00	12.06	1
13.00	13.07	1
14.00	14.06	1
15.00	15.06	1
16.00	16.07	1
17.00	17.06	1
17.00	17.07	2
16.00	16.06	2
15.00	15.07	2
14.00	14.07	2
13.00	13.08	2

Average difference 0.066 $\pm$ 0.008 cm.

b. Master Position 13.00 cm. Follower Position shown

Direction 1	Direction 2
13.06	13.08
13.07	13.08
13.07	13.08
13.07	13.08
13.08	13.08

Average 13.075 $\pm$ 0.007 cm

$$\frac{6.4}{0.058} \times 6.6 \times 10^{-4} = 7.3 \times 10^{-2} \text{ microwatts}$$

or 7.3×10^{-8} watts.

A series of neutral density filters were then introduced into the beam. It was found that a 1.2 density filter, corresponding to 16-fold attenutation, was compatible with tracking, but that a 1.5 filter, corresponding to 32-fold attenuation, inhibited tracking. The minimum power for tracking is therefore:

$$\frac{1}{16} \times 7.3 \times 10^{-8} = 4.5 \times 10^{-9} \text{ watts}$$

D. Space Communications Application of the Multiplication Effect

An attempt will be made in this section to extrapolate from the observed characteristics of the breadboard beam follower to a possible alignment device to be used in space communications. The breadboard beam follower is translational, whereas the displacement of an object at large distances is seen as angular motion. However, the two cases are comparable since in each case action is caused by the displacement of the image of the distant object on the photocell surface. In the beam follower, this is corrected by translational motion of the follower unit until the image is centered. In a space alignment device, the follower would be rotated until the image is again centered. This does not affect the calculation.

Possible applications of the alignment device would be space-to-ground, ground-to-space, or space-to-space. In each case a beacon at station A illuminates station B, moving with respect to A. A follower device on B keeps a receiver aligned with the beacon by turning it in consonance with the apparent angular motion of A as seen from B. A further possible application is when the beacon and follower are at the same station, and a moving object with a specularly reflecting surface is followed by tracking the beacon reflection.

Without loss of generality, we shall take the case of a beacon located on a communication satellite at a distance d from a ground station. Its tangential velocity with respect to the station is V. The beacon is a laser beam (continuous) of power P contained in a cone of angle α. Since $\alpha \ll 1$, the solid angle Ω is given by

$$\Omega = \alpha^2 \pi / 4$$

At the ground station the beam is intercepted by a lens or reflector of area A and focal length f which projects it on the surface of a photoconductor. We shall impose the restriction $A \leq f^2$ for a practical optical system. The velocity of motion of the beacon's image on the cell is ν and is given by

$$\nu = Vf/d.$$

The power per unit area at the receiver is

$$P/\Omega d^2$$

and the power p concentrated at the image is

$$p = 4AP/\alpha^2 d^2 \pi.$$

The minimum power required for the beacon is given by taking $A = f^2$:

$$P = \frac{p\alpha^2 d^2 \pi}{4f^2} = \frac{p\alpha^2 d^2 V^2 \pi}{4d^2 \nu^2} = \frac{p\alpha^2 V^2 \pi}{4\nu^2}$$

Note that the distance d cancels out.

We have measured the maximum velocity of translation of our master unit as 0.125 cm/sec. Since the distance from the pinhole in the master to the lens is 60 cm and the distance from lens to cell is 10 cm, the corresponding value for ν is:

$$\nu = 0.02 \text{ cm/sec} \quad (0.002 \text{ radians/sec})$$

We have also measured the minimum power input p required for tracking as:

$$p = 4 \times 10^{-9} \text{ watts}$$

We may also assume the following:

$d = 10^9$ cm (10,000 km, or about 6000 miles)

$V = 10^6$ cm/sec (6 miles/sec)

$\alpha = 10^{-3}$ (1 milliradian, a practical value for lasers)

We then obtain:

$$f = \frac{\nu d}{V} = \frac{2 \times 10^{-2} \times 10^9}{10^6} = 20 \text{ cm}$$

$$p = \frac{4 \times 10^{-9} \times 10^{-6} \times 10^{12} \times 0.78}{4 \times 10^{-4}} = 8 \text{ watts}$$

The alignment link thus requires a parabolic reflector of 8-inch focal length and about 9-inch diameter, and an 8-watt cw laser. The former is within the state of the art; the latter cannot at present be obtained in a visible wavelength. However, it should be noted that an improvement in collimation of the laser to 0.1 milliradian would reduce the required power to 0.08 watt. These numbers do not take account of losses due to transmission through the atmosphere and the inefficiency of the optical system.

It is anticipated that these alignment devices will work in pairs since it is necessary to keep the laser beam from one station aligned in order to activate the device at the other station.

The accuracy of alignment has also been measured. In our beam follower, the standard deviation of the position of the follower for a given position of the master was 7×10^{-3} cm (0.07 mm). This includes the random error in the manual positioning of the master; the correct value may be less. This may be taken as the standard deviation of the null position of the image on the photoconduc tor. Since the focal length of the lens was 10 cm, this deviation corresponds to 0.7 milliradians. This is less than the assumed value of α and it is therefore possible to use this device to train a laser beacon on the other station. This indicates that a paired alignment device arrangement is feasible.

V. CONCLUSIONS

The feasibility of utilizing the multiplication effect for alignment of light beams has been successfully demonstrated by the design, construction and operation of a breadboard beam follower. It should now be possible to evaluate the feasibility and desirability of the application of devices based on the multiplication effect to problems in space navigation and communication.

Considerable progress has been made toward a fundamental understanding of the effect. Experimentally, we have determined at least qualitatively the relationship between the multiplication factor and the following parameters:

a. Wavelength of incident light beams
b. Intensity of incident light beams
c. Applied field strength and polarity
d. Thickness of photocell
e. Area of light spot
f. Rise and decay times

All these parameters were studied to some extent during the period covered by the ITR. This report has included the results of further experiments with parameters b, c, d, and f.

With regard to incident intensities, it has been established that the multiplication factor is a maximum when the incident beams are approximately equal in intensity.

The polarity of the applied field has been shown to affect the multiplication factor; when the indium electrode was negative, the multiplication factor was significantly greater than when the cadmium sulfide surface was negative.

Difficulties in developing skill in cell fabrication techniques have inhibited progress in the cell thickness studies. However, the available data do suggest that the multiplication factor increases with decreasing thickness.

Finally, the multiplication effect seems to be accompanied by a decrease in rise time and an increase in decay time (with respect to single side illumination).

Progress was noted in developing a mathematical model of the multiplication effect; the model has been shown to be capable of generating multiplication factors as great as (and even greater than) the observed values. If the model is valid it should also generate the correct (i.e., in conformity with experiment) parameter dependences. The theoretical expression for the multiplication factor contains ten parameters. Some of these parameters, relate to the hypothetical charge carriers, viz; diffusion constant (D), mobility (μE), recombination constant (k), and surface concentration (c_o, c'_o); the values of these parameters are unknown. Because of the complicated relationship between the unknown charge-carrier parameters and the observed parameter dependences, the generation (from the model) of the correct dependences may be a more formidable problem then the generation of large values of the multiplication factor.

It appears that progress in the understanding of the photoconductive multiplication effect is now primarily limited by the narrow range of materials studied so far. Considerable technical knowledge has been gained in our experiments on doped polycrystalline cadmium sulfide photoconductors, and this has allowed us to make appreciable progress in the direction of practical applications. It now appears appropriate to investigate the effect in other materials, including especially those in which internal parameters (mobility, carrier lifetime) are known, so that theory and experiment can be correlated.

APPENDIX

ABSTRACTS OF PAPERS DELIVERED ON THE PHOTOCONDUCTIVE MULTIPLICATION EFFECT

A. From J. Opt. Soc. Am. 56, 557 (1966)

Photocurrent Multiplication in Cadmium Sulfide by Simultaneous Spot Illumination.* Raymond P. Borkowski, Aryeh H. Samuel, William M. Block, Irving Bleicher, and Daniel Grafstein, General Precision Aerospace Research Center, Little Falls, New Jersey. The current multiplication effect is the enhancement of the photocurrent which occurs when directly opposite points on the surfaces of a sandwich-type photocell, consisting of either undoped single-crystal or doped polycrystalline CdS, are simultaneously irradiated by spots of light. Values as high as 100 for the enhancement factor, which is the ratio of the photocurrent produced under simultaneous illumination to the arithmetic sum of the photocurrents produced by each spot separately, have been observed. The effect is absent when both spots illuminate the same surface or different points on opposite surfaces, or when both surfaces are entirely illuminated. The optimum effect is observed when: (1) the wavelength combination utilized is 6550-5180 Å; (2) an intermediate intensity of one light source is used, while maintaining the intensity of the other source constant; (3) low electric fields, approximately 100 V/cm or less are applied; (4) light spot areas of approximately 2×10^{-3} cm^2 are used; (5) both light spots are in coincidence. The effect is independent of the angle of incidence of either of the two beams. A model based on the diffusion of charge carriers explains the results in part but presently no complete theoretical analysis has been achieved.

B. From J. Opt. Soc. Am. 56, 1430 (1966)

Mathematical Model of Photoconductive Multiplication Effect.* Aryeh H. Samuel, Marvin J. Kornblau, and Raymond P. Borkowski, General Precision Aerospace Research Center, Little Falls, New Jersey. A simple mathematical model has been developed to describe

* Work sponsored by NASA-Electronic Research Center, Cambridge, Massachusetts.

the photoconductive multiplication effect in cadmium sulfide.

A differential equation for the charge carrier concentration was written which can, in principle, account for the observed dependence of the effect on wavelength, light intensity, and electric field. The equation can be solved analytically but numerical integration is required to obtain the multiplication factor. Parameter values have been assumed and varied in an attempt to match experimental results; the sensitivity of the multiplication factor to different parameter values will be discussed. This model would predict that the multiplication effect should be observed in all photoconductors; but by suitable choice of parameters the effect can be made negligible.